ENHANCING THE CORROSION RESISTANCE OF A COMMERCIAL MAGNESIUM ALLOY USING POLYANILINE COATING

Thesis submitted

by

ASIF A. BALOCH

May 2018

For the degree of Masters of Philosophy

College of Sciences and Engineering

James Cook University, Australia

STATEMENT OF ACCESS

I, the undersigned, the author of this thesis, understand that James Cook University will make it available for use within the University Library and, by microfilm or via other means, allow access to users in other approved libraries. I understand that, generally, theses have protection under the Copyright Act and wish to place no further restriction on access to this thesis.

May, 2018

_____ _____

Asif A. Baloch

DECLARATION

I declare that this thesis is my own work and has not been submitted in any form for another degree or diploma at any university or other institution of tertiary education. Information derived from the published or unpublished work of others has been acknowledged in the text and a list of references is given.

May, 2018

_____ _____

Asif A. Baloch

ELECTRONIC COPY

I, the undersigned, the author of this work, declare that the electronic copy of this thesis provided to the James Cook University Library is an accurate copy of the print thesis submitted, within limits of the technology available.

May, 2018

_____ _____

Asif A. Baloch

COPYRIGHT DECLARATION

I, the undersigned, the author of this work, declare that every reasonable effort has been made to gain permission and acknowledge the owners of copyright material. I would be pleased to hear from any copyright owner who has been omitted or incorrectly acknowledged.

May, 2018

Asif A. Baloch

ACKNOWLEDGEMENTS

I am grateful to my supervisor, Associate Professor Bobby Mathan for his unwavering support, advice and guidance through this research. I would also like to thank my co-supervisor Professor Yinghe He for his support.

I would like to thank my fellow postgraduate students R. Walter, O. Kazum, A. Abbasi and Dr R. Mohumed for their support and friendship.

A huge thank you to the staff of the College of Science and Engineering, especially Bio-Engineering and Materials Laboratory Technician Ruilan Liu, Academic Services Officer Melissa Norton and Dr Shane Askew, Senior Research Officer, Advanced Analytical Centre.

I sincerely thank my wife Huma Bahram and my children Paaris, Esfandyar and Savash for their understanding, love and encouragement through the tough times encountered during the production of this thesis. Finally, I would like to thank all of my family members for their words of encouragement and prayers.

STATEMENT ON THE CONTRIBUTION OF OTHERS

This thesis included contributions from the following people.

Research supervisory team:

Associate Professor Bobby Mathan (College of Science and Engineering, James Cook University)

Professor Yinghe He (College of Science and Engineering, James Cook University)

Editorial support:

Associate Professor Bobby Mathan

Dr. Mary Casolin

Dr. John Gibbens

ABSTRACT

Magnesium alloys are attractive materials for structural engineering applications due to their high strength-to-weight ratios and formability. However, the widespread use of magnesium alloys has been hindered by their poor corrosion resistance. Generally, magnesium alloys containing low amounts of impurities (iron and silicon) have acceptable atmospheric corrosion resistance, but the corrosion resistance deteriorates in chloride-containing environments.

Many surface engineering/coating techniques, such as electroplating, anodisation, micro-arc oxidation, chemical conversion and polymer coatings, have been studied to enhance the corrosion resistance of magnesium and magnesium-based alloys. However, in recent years, conducting polymers have gained high interest for use as corrosion protection coatings on engineering materials such as steel, copper and magnesium due to their unique electrical properties. Furthermore, these conducting polymers can be easily processed and are economically viable for use as metal coatings. Polyaniline and polypyrrole are the conducting polymers most commonly studied for use as coating materials for the corrosion protection of metals. In recent years, electrochemical polymerisation techniques have been widely used due to their characteristics of being environmentally friendly, easy to process, rapid and requiring few chemical additives. However, synthesis of polymer coatings is challenging when forming coatings on active metals, due to oxidation or prior dissolution of the metal substrate.

In this study, following cyclic voltammetry coating, the voltammetric curves for the alloy in the polyaniline sodium salicylate electrolyte (PASS) showed that the first-forward cycle had strong magnesium oxidation until ~0.75 V and, above that, oxidation of aniline started to occur. However, in subsequent forward cycles, magnesium oxidation was

insignificant due to the formation of polyaniline, which occurred during the reverse cycles. In contrast, in the polyaniline potassium hydroxide electrolyte (PAPH), which contained strongly alkaline potassium hydroxide, there was little dissolution of magnesium during the first-forward cycle. Based on the anodic peak current density, it can be said that the oxidation of aniline in PAPH electrolyte was significantly lower than in the PASS electrolyte. Further, it was noted that the peak current increased as the number of cycles increased in the PAPH electrolyte, which is in contrast to that observed in the PASS electrolyte. The corrosion rates of the bare metal, and the PASS- and PAPH-coated alloy samples were 2.02, 0.34 and 4.92 mpy, respectively. The degree of protection (DP) provided by the PASS coating was ~83%.

The second phase of coating testing was performed using the galvanostatic technique at current densities of 14, 18 and 20 mA/ cm^2. Potentiodynamic polymerisation tests of bare samples and samples coated with aniline and sodium salicylate were carried out in a chloride-containing solution. The corrosion tests showed substantial decreases in the corrosion currents of samples coated in aniline and sodium salicylate electrolyte. The systematic decrease in corrosion current revealed that the sample coated at 20 mA/cm^2 had better corrosion resistance than those coated at 18 and 14 mA/cm^2. The DPs of the samples coated at 20, 18 and 14 mA/ cm^2 were ~97%, ~48% and ~5%, respectively. The corrosion rates for the bare alloy and alloys coated at 14, 18 and 20 mA/cm^2 were 6.27, 5.96, 3.27 and 0.113 mpy, respectively. For all the samples, coating was carried out for 600 seconds. However, at high current densities and high coating times, samples started substantial hydrogen evolution. Severe bubble formation hindered the coating process, causing blisters in the coating.

Alkaline pre-treatment of the magnesium alloy prior to electropolymerisation of aniline was carried out to enhance corrosion resistance. Pre-treatment of the alloy was done in 3 M sodium hydroxide solution at constant potentials of −750mV and −195mV. Electropolymerisation was performed using a cyclic voltammetry technique in an acidic electrolyte containing aniline and sodium salicylate. The corrosion protection provided by the polyaniline coating on the alloy was evaluated using potentiodynamic polarisation in a chloride-containing solution. The electrochemical results showed that the polyaniline coating reduced the alloy's corrosion rate by almost an order of magnitude. However, post-corrosion analysis revealed delamination of the coating. It is suggested that polyaniline did not adhere well to the hydroxide/oxide layer that formed on alloys during pre-treatment.

This study found that aniline, as a conducting polymer, formed better coatings in acidic electrolytes than in alkaline ones. The propagation of aniline in the emeraldine state (dark green colour coating) produced good coatings on the surfaces of magnesium alloy samples. The coating obtained at 20 mA/cm^2 by the galvanostatic technique provided the highest corrosion protection. However, at current densities higher than 20 mA/cm^2, hydrogen evolution hindered coating formation. The effect of coating time is also important in the galvanostatic coating technique; hydrogen evolution increased with coating time. Alkaline pre-treatment of magnesium alloy did not enhance the coating morphology. During potentiodynamic polarisation tests, polyaniline coatings tended to peel off due to weak adhesion with the metal substrate. The outcomes of this study may help improve the coating quality of magnesium alloy used in small gadgets and automotive industry. However, there is still more work needs to be done to form pore free coating on the metal for commercial use.

The findings from this dissertation have been disseminated through the following publications.

Publications:

- Asif Baloch and M. Bobby Kannan "Electropolymerisation of aniline on AZ91 magnesium alloy: Effect of coating electrolyte corrosiveness" *Metals* **2017**, *7*(12), 533; doi:10.3390/met7120533
- Asif Baloch and M. Bobby Kannan. "Galvanostatic polymerisation of aniline on AZ91 magnesium alloy: Evaluating the corrosion protection behaviour in chloride-containing solution" (In preparation)

Conference Paper:

- Asif Baloch and M. Bobby Kannan "Electropolymerisation of aniline on alkaline pre-treated magnesium alloy and corrosion evaluation" ACA Conference "Corrosion & Prevention 2017" Sydney, 12-15 November 2017.

TABLE OF CONTENTS

Statement of Access iii

Statement on Sources iv

Electronic Copy v

Copyright Declaration vi

Acknowledgement vii

Statement on the Contribution of Others viii

Abstract ix

Table of Contents xiii

List of Figures xvi

List of Tables xix

List of Symbols xx

CHAPTER 1: Introduction 1

1.1 Background 1

1.2 Objectives 2

CHAPTER 2 Literature Review 4

2.1 Magnesium 4

2.2 Corrosion 6

2.3 Potentiodynamic Polarisation Method 8

2.4 Types of Corrosion 9

2.4.1 Uniform corrosion 9

2.4.2 Localised corrosion 10

2.4.3 Pitting corrosion 11

2.4.4 Galvanic corrosion 12

2.4.5 Crevice corrosion 14

2.4.6 Intergranular corrosion 16

2.4.7 Stress corrosion cracking (SCC) 16

2.5 Conducting Polymer 17

2.5.1 Polylaniline 19

2.5.2 Polypyrrole 21

2.5.3 Polythiophene 22

2.6 Electropolymerisation 23

2.7 Electropolymerisation Techniques 25

2.7.1 Galvanostatic 25

2.7.2 Potentiostatic 29

2.7.3 Cyclic voltammetry 30

2.8 Effect of Electrolyte pH 32

2.9 Effect of Coating Time 33

CHAPTER 3 Materials and Experimental Procedure 38

3.1 Material.....38

3.2 Electropolymerisation 38

3.2.1 Cyclic voltammetry method 39

3.2.2 Galvanostatic method 40

3.3 Coating Characteristics 41

3.3.1 Microscopic analysis 41

3.3.2 Coating thickness 41

3.3.3 Coating adhesion 41

3.3.4 Scanning electron microscopy (SEM) 42

3.3.5 Fourier transform infrared spectroscopy (FTIR) 42

3.4 Corrosion Testing 42

CHAPTER 4 Electropolymerisation of Aniline on AZ91 Magnesium Alloy: The Effect of Coating Electrolyte Corrossiveness 45

4.1 Electrolyte Behaviour and Corrossiveness 45

4.1.1 Effect of pH on metal substrate 46

4.1.2 Post corrosion optical microscopic analysis without polyaniline coating ..48

4.2 Polymer Coating 49

4.2.1 Optical microscopic analysis of polyaniline coated sample. 51

4.2.2 Coating thickness and FTIR analysis 52

4.3 Potentiodynamic Polarisation 53

4.3.1 Post corrosion analysis 54

4.4 Reaction Mechanism of Aniline 56

4.5 Summary 58

CHAPTER 5 Galvanostatic Polymerisation of Aniline on AZ91 Magnesium Alloy: Evaluating The Corrosion Protection Behaviour in Chloride-Containing Solution 59

5.1 Galvanostatic Coating 59

5.1.1 Effect of current density at 14,18 and 20 mA/cm^2 59

5.1.2 Coating morphology at different current densities 61

5.1.3 FTIR analysis at different current densities 62

5.2 Potentiodynamic Polarisation 62

5.3 Summary 66

CHAPTER 6 Electropolymerisation of Aniline on Alkaline Pre-treated AZ91 Magnesium Alloy and Corrosion Evaluation 67

6.1 Magnesium Passivation 67

6.1.1 Potentiostatic passivation 68

6.2 Cyclic Voltammetry Coating on Pre-treated AZ91 Magnesium Alloy Samples 69

6.3 Corrosion Analysis 70

6.3.1 Potentiodynamic polarisation test 70

6.3.2 Macroscopic analysis 72

6.3.3 Coating delamination mechanism 72

6.4 Summary 74

CHAPTER 7 Conclusions 75

References 77

LIST OF FIGURES

Figure 2.1 (A) Equilibria of Mg-H_2O system in presence of H_2 at 25 °C (B) Schematic presentation of the three-layer structure of the oxide films on Mg.……7

Figure 2.2 A typical potentiodynamic polarisation curve ……8

F**igure 2.3** Typical surface appearances of ultra-high-purity Mg specimens showing uniform corrosion,……..9

Figure 2.4 Photographic images showing the influence of immersion time of the appearance of a corroding AZ31 surface held in aerated 5% w/v NaCl (aq) electrolyte at pH 7 for (a) 10, (b) 30, (c) 60 and (d) 120 min 10

Figure 2.5 SEM micrographs of AZ80 magnesium alloy after immersion in 0.5 wt.% NaCl solution for 4 h immersion 11

Figure 2.6 Appearance of HP Mg and carbon steel galvanic corrosion couple, (a) overview in 3.5% NaCl saturated with $Mg(OH)_2$ after 2 days immersion, showing white ring of corrosion products on the HP Mg surrounding the steel insert, (b) overview of specimen after 6 day immersion and removal of corrosion products, (c) enlarged view of central area of (b). 12

Figure 2.7 (A) Two typical mounted HP Mg specimens exposed to the 3.5% NaCl saturated with $Mg(OH)_2$ solution. (B) SEM views appearance of crevice corrosion for the encapsulated Mg samples. Typical samples were extracted from the encapsulation after immersion tests and the HP Mg surface was examined inside the crevice between the Mg metal and the encapsulation..... 14

Figure 2.8 SEM image of magnesium alloy ZE41 tested in distilled water at ambient temperature. 15

Figure 2.9 Stress corrosion cracking, corrosion of friction stir welded (FSW) AZ31 Mg alloy tested at slow strain rate tensile (SSRT) test method. 16

F**igure 2.10** Conducting polymers: (a) polyaniline (PAni) (b) polythiophen (PThio) and (c) polypyrrole (PPy) 18

Figure 2.11 Electropolymerisation mechanism of aniline to polyaniline 19

Figure 2.12 Electropolymerisation mechanism of three oxidations states of aniline. 20

Figure 2.13 Galvanostatic curves of polyaniline coating on steel under different electrolyte bath conditions..... 26

Figure 2.14 Potentiodynamic polarisation curves of Cp Mg in different ionic liquids at 60 °C. 27

Figure 2.15 3D topographical images of MAO coatings prepared at different current densities: (a) 0.026 A/cm^2 "P1", (b) 0.046 A/cm^2 "P2" and (c) 0.067 A/cm^2 "P3" coatings respectively……..... …...28

Figure 2.16 Potentiodynamic polarisation curves of PANI coated AA1100 and bare AA1100 in 0.5 M NaCl solution 29

Figure 2.17 Cyclic voltammetry test on polyaniline, performed in different electropolymerization conditions: (a) effect of different scan rates, (b) effect of different switching potentials. 30

Figure 2.18 The voltammogram for the electrochemical synthesis of PANI (0.1 M pyrrole and 0.3 M oxalic acid) solution coating on steel. 31

Figure 2.19 The polarisation curves of as-plated nickel–phosphorus alloy from a bath containing sodium hypophosphite and glycin– citrate complexing agents, tested in 3.5% NaCl solution. 33

Figure 3.1 Schematic of a three-electrode cell used for electrochemical experiments.....38

Figure 4.1 Potentiodynamic polarisation curves of AZ91 magnesium alloy in 0.25M potassium hydroxide and 0.1 M sodium salicylate electrolytes. 46

Figure 4.2 Optical micrographs of AZ91 magnesium alloy after potentiodynamic polarization experiments in: (a, b) 0.25M potassium hydroxide and (c, d) 0.1M sodium salicylate. 47

Figure 4.3 Cyclic voltammetry response of AZ91 magnesium alloy in PASS (aniline + sodium salicylate) and PAPH (aniline + potassium hydroxide) electrolytes. 49

Figure 4.4 Optical micrographs of the coated AZ91 magnesium alloy: (a, b) PAPH coated, and (c, d) PASS coated. 51

Figure 4.5 FTIR analysis of PASS and PAPH coatings. 52

Figure 4.6 Potentiodynamic polarization curves of the bare metal and coated AZ91 magnesium alloy samples in chloride-containing solution. 53

Figure 4.7 Post-corrosion macrographs of AZ91 magnesium alloy: (a) bare metal, (b) PASS coated, and (c) PAPH coated, after potentiodynamic polarization in chloride containing solution…… 54

Figure 4.8 Electropolymerisation mechanism of aniline to polyaniline……..... 56

Figure 5.1 Galvanostatic response of AZ91 magnesium alloy in 0.3 M aniline and 0.1 M sodium salicylate solution 59

Figure 5.2 SEM micrographs of coated samples of (a) 14 mA/cm^2 (b) 18 mA/cm^2 (c) 20 mA/cm^2 before potentiodynamic polarization test. 60

Figure 5.3 Fourier Transform Infrared (FTIR) analysis of polyaniline coating on AZ91 magnesium alloy at 14, 18 and 20mA/cm^2 current densities 61

Figure 5.4 Potentiodynamic polarization curves of bare and coated AZ91 magnesium alloy samples in chloride-containing solution. 63

Figure 5.5 Degree of protection of the samples coated at 14, 18 and 20 mA/cm ^{2} current densities. 64

Figure 6.1 Poubaix diagram of magnesium showing the corrosion and passivation at different pH level. 66

Figure 6.2 Transient potential graph of 3 M sodium hydroxide pre-treatment of magnesium alloy AZ91. 67

Figure 6.3 Macrograph of (a) bare sample (b) -750 mV and (c) -195 mV pre-treated in 3 M sodium hydroxide solution. 68

Figure 6.4 Cyclic voltammetry curves of alkaline pre-treated AZ91 magnesium alloy in 0.3 M aniline and 0.1 M sodium salicylate solution 68

Figure 6.5 Potentiodynamic polarization curves of AZ91 magnesium alloy 3 M NaOH pre-treated and untreated sample coated with aniline and tested in 0.5 g/l sodium chloride solution. 70

Figure 6.6 Microscopic images of sample (a) before (b) after potentiodynamic polarization of the sample pretreated in sodium hydroxide 3 M and coated in 0.1 aniline and 0.3 M sodium salicylate. 71

Figure 6.7 Schematic diagram of corrosion attack mechanism on AZ91 magnesium alloy sample coated with 0.1 aniline and 0.3 M sodium salicylate electrolyte. 71

Figure 6.8 Schematic diagram of corrosion attack mechanism on AZ91 magnesium alloy sample 3 M NaOH pre-treated and coated with 0.1 aniline and 0.3 M sodium salicylate electrolyte. 72

LIST OF TABLES

Table 2.1 Alloy elements for magnesium and their properties effects 5

Table 2.2 Standard electromotive force (emf) series of metals 13

Table 2.3 DC polarisation results of the coating effect at different pH polypyrrole and poly(N-methylpyrrole) coatings. 25

Table 2.4 Corrosion current density, corrosion potential and corrosion rates of bare and phosphated steel in 3.5 % NaCl solution. 33

Table 2.5 EIS results for zinc phosphate coated steel samples at 4 mA/cm^2 at 20. 40 and 60 min in 3.5 % NaCl solution 34

Table 2.6 Summary of the literature of corrosion prevention by using conducting polymer on different alloy. 35

Table 2.7 Summary of the literature of corrosion prevention by using different coatings on magnesium alloy. 36

Table 3.1 Chemical composition of the magnesium alloy used in the study..... 37

Table 4.1 Electrochemical corrosion data of AZ91 magnesium alloy in two different electrolytes. 47

Table 4.2 Thickness and adhesion of the coatings formed on AZ91 magnesium alloy in two different electrolytes 50

Table 4.3 Electrochemical corrosion data of the bare metal and coated AZ91 magnesium alloy in chloride-containing solution. 53

Table 4.4 The pH of the coating electrolytes and variations in the pH of the corrosion test solution. 55

Table 5.1 Thickness of polyaniline coating at 14, 18 and 20 mA/cm^2 current densities in 0.3 M aniline and 0.1 sodium salicylate.. 62

Table 5.2 Effect of the coating applied currents of the galvanic technique on the corrosion parameters of AZ91 magnesium alloy in 0.5g/l NaCl obtained from the potentiodynamic experiments. 63

Table 6.1 Effect of the corrosion containing environment and degree of coating protection on bare, without pre-treatment and pre-treated coating on AZ91 magnesium alloy in 0.5g/l NaCl. ..... ….70

LIST OF SYMBOLS

Wt.%	=	Weight in percentage
CR	=	Corrosion rate
ρ	=	Density of the metal in g/cm^3
SiC	=	Silicon-carbide
SEM	=	Scanning electron microscope
FTIR	=	Fourier transform infrared spectroscopy
OCP	=	Open circuit potential
E_{corr}	=	Corrosion potential
i_{corr}	=	Corrosion current density
DP	=	Degree of protection

CHAPTER 1 Introduction

1.1 Background

Magnesium alloys are attractive materials for structural engineering applications due to their high strength-to-weight ratio and formability (Dobrzanski et al., 2007; Hirsch & Al-Samman, 2013; Luo et al., 2013;). However, the widespread use of magnesium alloys has been hindered due to their poor corrosion resistance (Easton et al., 2008; Kulekei et al., 2008; Mordike & Ebert, 2001). Generally, magnesium alloys containing low amounts of impurities (e.g. iron and silicon) have acceptable atmospheric corrosion resistance, but this deteriorates in chloride-containing environments (Easton et al., 2008; Mordike & Ebert, 2001).

A popular magnesium alloy containing aluminium and zinc as alloying elements is AZ91. The literature suggests that the corrosion rate of AZ91 increases with chloride-ion concentration and is also dependent on the pH of any electrolytes it comes into contact with (Easton et al., 2008). For example, in acidic solution (pH = 2), the concentration of chloride ions does not affect the corrosion rate of AZ91 magnesium alloy; however, in alkaline solution, the chloride ion concentration influenced the corrosion rate of AZ91 magnesium alloy (Easton et al., 2008). Feng et al. (2013) reported that for AZ91 magnesium alloy, the thickness of the magnesium hydroxide passive film increases with increase in the electrolyte pH from 9 to 11, which consequently decreases the alloy's corrosion rate. They also found that hydrothermal treatment influences the corrosion resistance of this alloy.

Surface engineering/coating techniques such as electroplating, anodisation, micro-arc oxidation, chemical conversion and polymer coatings have been studied for enhancing the corrosion resistance of magnesium and magnesium-based alloys (Craig 1998;

CSIRO, 2015; Fontana, 1987; Gospondinova & Terlmezyan, 1998; Ghali, 2004, 2010; Rajan et al., 2000; Schab-balcerzak, 2011). However, in recent years, conducting polymers have gained much interest for use as corrosion protection coatings on engineering materials, such as steel, copper and magnesium, due to their unique electrical properties compared to non-conductive coating of chromates and phosphates. (Breslin et al., 2005; Camalet et al., 2000; Hongbin et al., 2011; Masdarolomoor 2006; Sapurina & Shishoy 2012). The growing environmental concerns have restricted the use of chromate and phosphate containing materials for coatings applications. Furthermore, these conducting polymers can be electrochemically processed which make these polymers economically and chemically viable by using minimal chemical additives. These conducting polymer coatings provide excellent protection to the complex frames of small gadgets such as cameras, mobile phones, laptops, and everyday small tools.

Polyaniline and polypyrrole are the most popular conducting polymers studied as coating materials. Iroh and Wencheng (2000) coated low carbon steel with polypyrrole by an electrochemical method. They reported that coatings formed at relatively low current densities exhibited higher corrosion resistance than those prepared at higher current densities. Similarly, Kazum and Kannan (2013) reported that electropolymerization of aniline on steel at 20 mA/cm^2 produced a polyaniline coating that performed better in chloride-containing solution than one formed at 30 mA/cm^2. They suggested that at higher applied currents, the inevitable hydrogen evolution hinders the formation of coatings. However, Pawar et al. (2006) reported that a uniform and strongly adherent polyaniline could be formed on mild steel using a cyclic voltammetry coating technique.

1.2 Objectives

Electropolymerisation on a highly reactive metal such as magnesium is challenging, since the metal may dissolve during the coating process if the electrolyte used is corrosive. To overcome this problem, this study aims to increase the corrosion resistance of AZ91 magnesium alloy during the polymer coating process.

The main research objectives of this study were to:

- Electropolymerise aniline on AZ91 magnesium alloy using acidic and alkaline electrolytes
- Optimise the cyclic voltammetry and galvanostatic parameters of the coating process
- Examine the effect of alloy pre-treatment on aniline electropolymerisation

CHAPTER 2 Literature Review

2.1 Magnesium

Magnesium is commonly used in many engineering applications because of its light weight and high specific strength. This makes it attractive for high pressure die-casting and milling/turning at high speed. Magnesium has good weldability under a controlled atmosphere, is corrosive-resistant, and has good electrical and thermal conductivity. Pure magnesium is generally alloyed with elements such as aluminium, zinc, copper, manganese, rare earths (cerium, praseodymium, thorium, yttrium) and zirconium to enhance its mechanical properties and corrosion resistance (Dobrzanski et al., 2007; Easton et al., 2008; Hirsch et al., 2013; Luo, 2013; Mordike & Ebert; 2001).

Table 2.1 Elements commonly used for magnesium alloying and their properties (International Magnesium Association)

Alloying Element	Properties
Aluminium	• Increases hardness, strength and castability • Average alloy contains about 2–9 wt. % of aluminium. Can be heat-treated with greater than 6 wt. % aluminium • High amount of aluminium decreases the ductility of the alloy
Zinc	• Increases alloys' fluidity in casting • Improves resistance to corrosion when added to magnesium alloys with nickel and iron impurities. • Additions of 2 wt. % or higher improve hot-cracking
Calcium	• Improves thermal and mechanical properties and assists in grain refinement and creep resistance • Reduces oxidation during processing • Allows for better elasticity of sheet metal • Higher than 3 wt. % increases the risk of cracking during welding
Cerium	• Improves corrosion resistance • Increases plastic deformation capability, magnesium elongation and work hardening rates • Reduces yield strength
Manganese	• Increases resistance to corrosion in aluminium containing alloys • Reduces the adverse effects of iron
Rare earths	• Increase high temperature creep, corrosion resistance and strength • Allow lower casting porosity and weld-cracking in processing
Silicon	• Increases fluidity • Improves creep resistance • Used in pressure die-casting
Tin	• When added to aluminium, improves ductility and reduces tendency to crack during processing
Zirconium	• Refines grain size in sand and gravity castings (not combined with aluminium)

Magnesium alloys have various applications in the automobile and aircraft industries as they contribute to fuel efficiency. Their high strength-to-weight ratio is the prime reason for considering magnesium alloys as substitutes for aluminium and steel. Besides their use in the transport industry, magnesium is increasingly in demand for construction, electronics, medical equipment and bio-implants. Magnesium alloys are also widely used in many everyday gadgets (camera bodies, laptop frames, smartphone casings, portable media devices, small tools for home use, gardening tools, bicycle frames, golf and tennis rackets; Luo, 2013). High pressure die-casting (HPDC), sand-casting and investment casting are the commonly used procedures for the production of magnesium alloys (Dobrzanski et al., 2007; Luo, 2013).

In automobile manufacturing, magnesium has largely replaced steel and aluminium in products such as gearbox housings, crankcases, steering wheels, sealing flanges, steering column lock housings, airbag housings, seat frames, wheels and suspension arms (Mark et al., 2008; Mustafa, 2008). Magnesium is also widely used in the aircraft industry, in both commercial carriers and military aircraft.

2.2 Corrosion

Corrosion can be defined as the destruction or deterioration of a material because of reaction with its environment (Fontana, 1986). In Australia, the annual cost of corrosion is estimated to be A$1.3 billion, since the major metropolitan cities of Australia are situated along a coastal belt (CSIRO, 2015). Corrosion of magnesium is one of the key issues in its growing worldwide market. Magnesium is especially prone to corrosion in chloride-containing environments. In an aqueous solution, magnesium rapidly oxidises and forms a passive layer of $Mg(OH)_2$ (Ghali et al., 2004). The corrosion reactions of magnesium in an aqueous environment are given below:

Anodic reaction (oxidation):

$$Mg \rightarrow Mg^{2+} + 2e \qquad (2.1.1)$$

Cathodic reaction (reduction):

$$2\,H_2O + 2e \rightarrow 2\,OH^- + H_2 \qquad (2.1.2)$$

Product formation:

$$Mg^{2+} + 2OH^- \rightarrow Mg(OH)_2 \qquad (2.1.3)$$

Overall reaction:

$$Mg + 2H_2O \rightarrow Mg(OH)_2 + H_2 \qquad (2.1.4)$$

Magnesium hydroxide film is not stable in chloride-containing environments Figure 2.1.

The reaction that occurs is shown below (Ranjan et al., 2000)

$$Mg(OH)_2 + 2Cl \rightarrow Mg(Cl)_2 + 2OH^- \qquad (2.1.5)$$

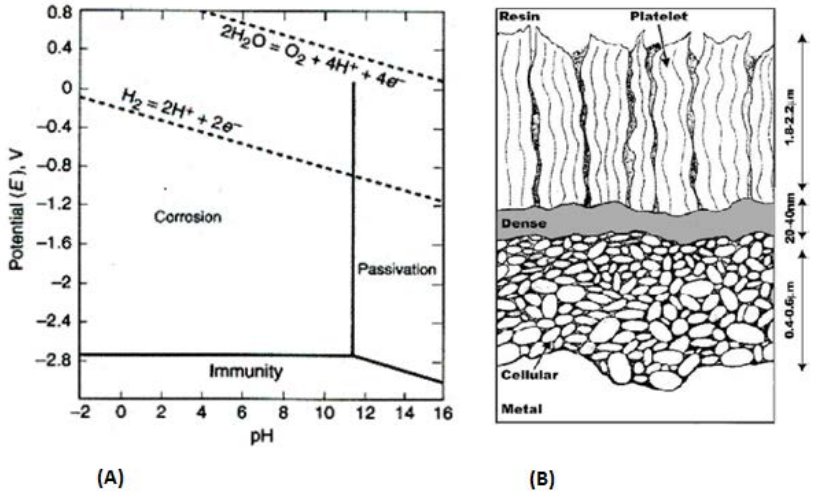

Figure 2.1 (A) Equilibria of Mg-H_2O system in presence of H_2 at 25 °C; (B) schematic representation of the three-layered structure of oxide film on Mg (Ghali, 2010).

2.3 Potentiodynamic polarization method

Potentiodynamic polarisation is a widely used technique to measure the corrosion current icorr to determine the corrosion rate of metals and alloys. This technique provides information regarding the passivation and localized corrosion behavior of metals and alloys in a given environment. In this method the applied potential is scanned through range of value to record the resultant induced current. In the anodic polarisation, the potential can be swept through the anodic direction from the corrosion potential (E_{corr}) value. At the anodic polarisation curve passivation and pitting susceptibility of the material may be presented. While in the cathodic polarisation the potential is swept through the cathodic direction from the E_{corr}. In the cathodic curve, cathodic reaction such as hydrogen evolution becomes dominant. The intersection of the cathodic and anodic curves is known as the corrosion potential (E_{corr}). The intersection of the linear region, otherwise known as the Tafel region, provides an estimation of the corrosion current density (i_{corr}). The corrosion current is proportional to the corrosion rate CR from the following equation (www.gamry.com, Yang 2008): . A typical polarisation curve is shown in Figure 2.1.

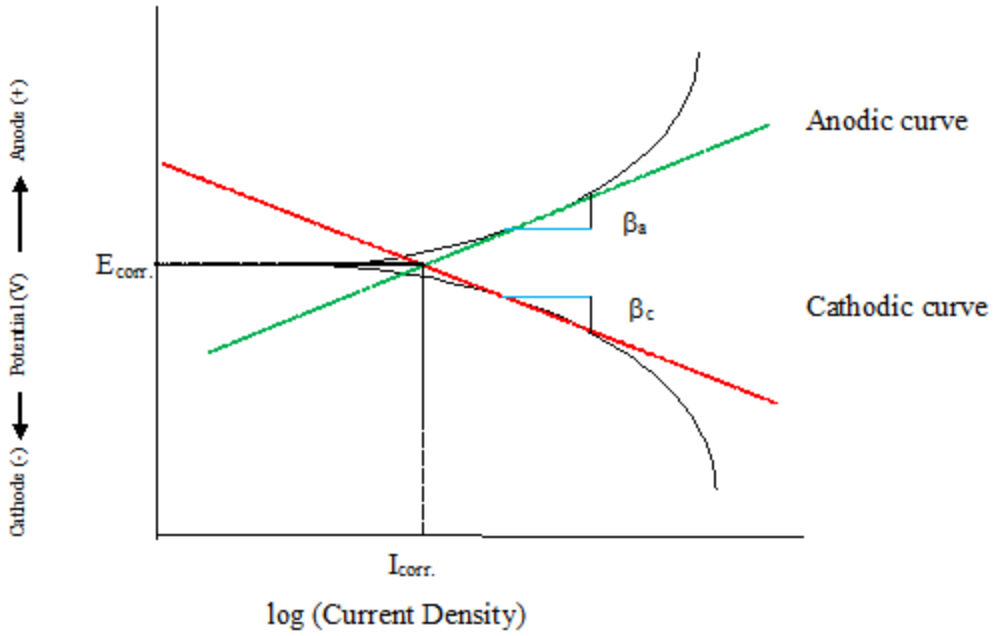

Figure 2.2 A typical potentiodynamic polarisation curve.

2.4 Types of Corrosion

Broadly, corrosion in metallic materials can be classified into two types: uniform and localised corrosion. The main sub-classifications of localised corrosion are described in this section. Magnesium and its alloys are generally prone to both uniform and localised corrosion.

2.4.1 Uniform Corrosion

Uniform corrosion is the most common type of corrosion seen in many metallic materials which do not show any passivation. This type of corrosion can occur in materials exposed to humid or aqueous environments. The consequence of this type of corrosion is thinning of the material. Hence, the deterioration rate of the material can be calculated by measuring the loss in material thickness. It is relatively easy to detect uniform corrosion since this type of corrosion can be visualised by the naked eye. Typically, coatings and corrosion inhibitors are used to protect materials from uniform corrosion. Uniform

corrosion was evident at the surface of an ultra-high-purity magnesium sample exposed to 3.5 Wt. % NaCl at the open circuit potential (OCP) for 14 days (Fuyong et al., 2016; Figure 2.3). The rate of localised corrosion was found to be somewhat higher than the rate of uniform corrosion. Uniform corrosion occurs due to a very unstable $Mg/Mg(OH)_2$ protective layer, especially in ultra-high-purity magnesium samples.

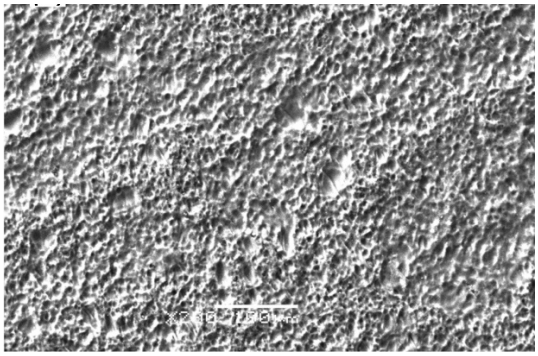

Figure 2.3 Typical surface appearance of ultra-high-purity Mg specimen showing uniform corrosion (Cao et al., 2016)

2.4.2 Localised Corrosion

Unlike uniform corrosion, the amount of metal dissolved during localised corrosion is much lesser. However, the effects of localised corrosion can be catastrophic. There are different types of localised corrosion, such as pitting, galvanic, intergranular and stress corrosion cracking. The material's properties, the shape of the component and environmental influences affect the susceptibility of the material to localised corrosion. A corroding surface shortly after breakdown is shown in Figure 2.4 B. a, which gradually becomes subject to localised corrosion after two hours of immersion in 5% w/v NaCl (Figures 2.4 B, b-d). Since a large area of the material comes under localised corrosion attack, bubble formation (hydrogen evolution) can be seen initiated at various locations of the surface. However, the location of the bubble formation was changing with time. Figure 2.4A, interpret the schematic diagram of proposed mechanism of AZ31 localised

corrosion reconciled with a scanning vibrating electrode (SVET) derived normal current density profile.

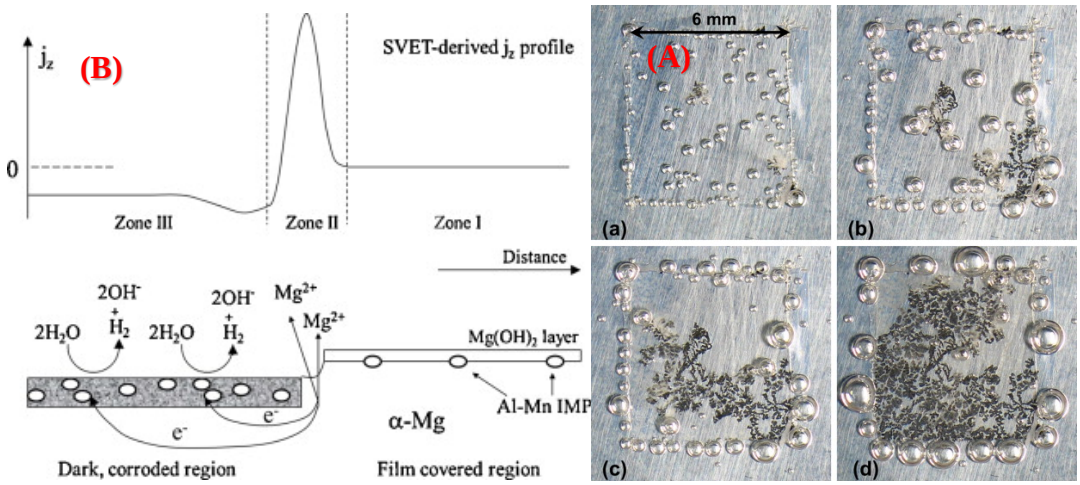

Figure 2.4 (A) Schematic diagram showing proposed mechanism of AZ31 localised corrosion reconciled with a typical SVET-derived normal current density profile. **Figure 2.4 (B)** Photographs showing the influence of immersion time on the appearance of a corroding surface of AZ31 alloy immersed in aerated 5% w/v NaCl (aq) electrolyte at pH 7 for (a) 10, (b) 30, (c) 60 and (d) 120 min (Williams et al., 2013)

2.4.3 Pitting Corrosion

Pitting corrosion is considered to be the most destructive type of corrosion, and produces extensive pores and holes in specific areas of localized corrosion. In this type of corrosion, the metal under attack develops small pits and cavities. This type of corrosion is hard to predict due to the small pore size and, often, these pores are coved under corrosion products (rust). These pits on the metal's surface generally appear as cavities due to the gradual dissolution of the metal. The Scanning Electron Microscopy (SEM) image in Figure 2.5 shows AZ80 magnesium alloy immersed for 4 hours in 0.5 wt. % NaCl. It exhibits pitting corrosion and corrosion attack along the grain boundaries, which perhaps show two different mechanisms: first, the grains were dissolved completely

during the corrosion process and, secondly, ongoing attack along the grain boundaries caused grains to fall out of the material.

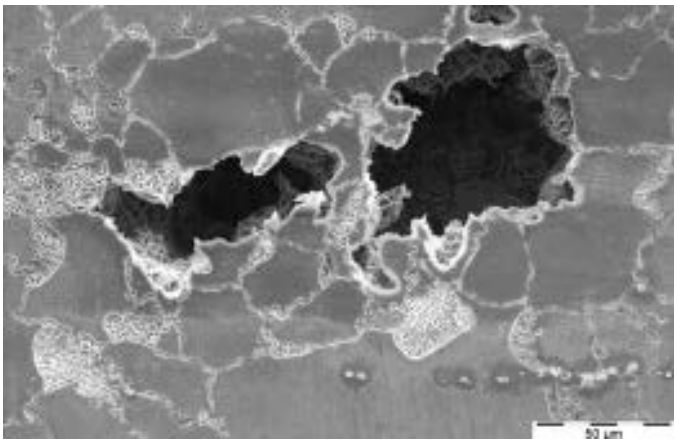

Figure 2.5 SEM micrographs of AZ80 magnesium alloy after immersion in 0.5 wt. % NaCl solution for 4 h (Bobby & Dietzel, 2012)

2.4.4 Galvanic Corrosion

Galvanic corrosion takes place when two different metals with different electrochemical potentials come in contact in a conductive environment. A corrosion reaction occurs when electrons flow between metals from two different electromotive force (emf) series. This depends upon factors such as the aggressiveness of the corrosive solution, the distance between the electrodes, and the contact area of the two metals. Prevention of this form of corrosion requires selection of metals which do not have electrode potentials with different emf values. Coatings and insulation can also help prevent galvanostatic corrosion with appropriate selection of the contact area between the two metals. Figure 2.6 shows the attendance of a galvanic couple when a stainless steel shaft (100 mm × 100 mm plate of high purity Mg with a central 20 mm diameter steel insert) for the galvanic couple is immersed in 3.5% NaCl solution. The figure reveals that a significant loss of Mg is evident at the steel-Mg interface. The loss of the magnesium material has two distinct features. One is that the loss in the area surrounding the coupling is severe but

decreases with distance from the steel-Mg interface. The other is that heterogeneous metal loss accrues as pits of various depths that are deeper near the area of the steel-Mg interface. The different shapes and sizes of pits are due to heterogeneous corrosion.

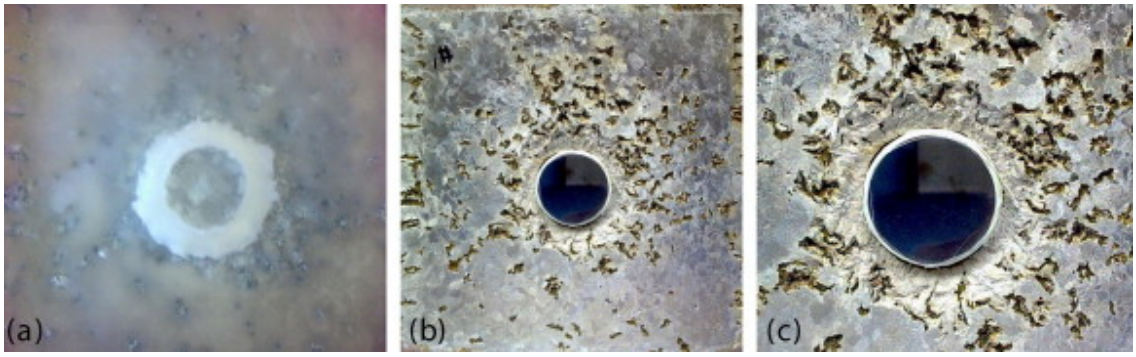

Figure 2.6 Appearance of a HP Mg and carbon steel galvanic corrosion couple: (a) overview in 3.5% NaCl saturated with $Mg(OH)_2$ after 2 days' immersion, showing a white ring of corrosion products on the HP Mg surrounding the steel insert, (b) overview of specimen after 6 days' immersion and removal of corrosion products, (c) enlarged view of the central area of (b) (Shi et al., 2012)

The common practice of preventing the galvanic corrosion is to carefully select the design materials which in general are close together in electromotive force (emf). The electromotive force (emf) for noble/cathodic and active/anodic metals are shown in Table 2.2.

Table 2.2 Standard electromotive force (emf) series of metals (Fontana, 1987)

	Metal-metal ion equilibrium	Electrode potential vs. normal hydrogen electrode at 25 °C (V)
Noble or cathodic ↑	$Au-Au^{3+}$	+1.498
	$Pt-Pt^{2+}$	+1.2
	$Pd-Pd^{2+}$	+0.987
	$Ag-Ag^{+}$	+0.799
	$Hg-Hg_2^{3+}$	+0.788
	$Cu-Cu^{2+}$	+0.337
	H_2-H^{+}	0.000
	$Pb-Pb^{2+}$	-0.126
	$Sn-Sn^{2+}$	-0.136
	$Ni-Ni^{2+}$	-0.250
	$Co-Co^{2+}$	-0.277
	$Cd-Cd^{2+}$	-0.403
	$Fe-Fe^{2+}$	-0.440
	$Cr-Cr^{3+}$	-0.744
	$Zn-Zn^{2+}$	-0.763
Active or anodic ↓	$Al-Al^{3+}$	-1.662
	$Mg-Mg^{2+}$	-2.363
	$Na-Na^{+}$	-2.714
	$K-K^{+}$	-2.925

2.4.5 Crevice Corrosion

Crevice corrosion is a form of severe localized corrosion that occurs under crevices and other shielded areas. This type of corrosion occurs in oxygen-confined spaces and cracks

where the flow of corrosive solution is restricted. It usually occurs on metal surfaces, especially under gaskets, lap joints, surface deposits, and bolt and rivet heads. Narrow spaces between metal-non-metal or metal-metal surfaces, and under biofouling (algae etc.), mud, and dirt deposits on metals submerged in seawater are major sites of crevice corrosion. Crevice corrosion is an oxygen-dependent phenomenon and in a confined crevice environment, the metal continues to corrode at a very limited scale, even after complete oxygen consumption within confined spaces. Figure 2.7 (A) shows mounted high purity Mg samples, while (B) shows a SEM image of a sample corroded in 3.5% NaCl solution. The results reveal that the mounted HP Mg sample was attack of crevice corrosion in the mounted samples. The crevice corrosion also shows some cracks at the surface of the sample. In the concluding remarks, the authors suggested that based on prior research, there was no evidence of crevice corrosion in Mg.

$$M^+ Cl^- + H_2O = MOH \downarrow + H^+ Cl^- \qquad (2.1.6)$$

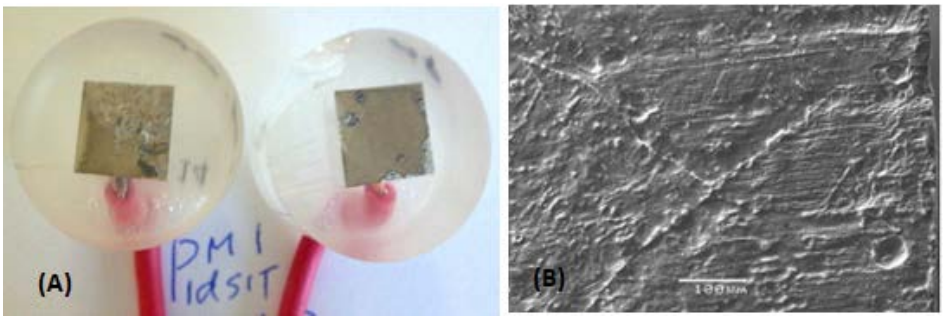

Figure 2.7 (A) Two typical mounted HP Mg specimens exposed to 3.5% NaCl saturated with $Mg(OH)_2$ solution. (B) SEM view of crevice corrosion in encapsulated Mg samples. Typical samples were extracted from the encapsulation after immersion tests and the HP Mg surface was examined inside the crevice between the Mg metal and the encapsulation (Atrens et al., 2011).

2.4.6 Intergranular Corrosion

Intergranular corrosion is a common form of localised corrosion and occurs at, or adjacent to, the grain boundaries of alloy metals; however, the bulk of the grains are unaffected. This type of corrosion occurs due to a potential difference between grains and grain boundaries. The intermetallic positive potential difference between grain boundaries and grains shows a cathodic behaviour towards the matrix, which creates a local cell. Intergranular corrosion can be prevented by adding elements which can stabilise the matrix during alloying, and by lowering the percentage of alloying elements prone to producing precipitation. Figure 2.8 reveals the intergranular corrosion of ZE41 alloy in distilled water. The image shows that the second phase particles, i.e. zirconium, zinc and rare-earths, initiate micro-galvanic corrosion along the grain boundaries in the sample.

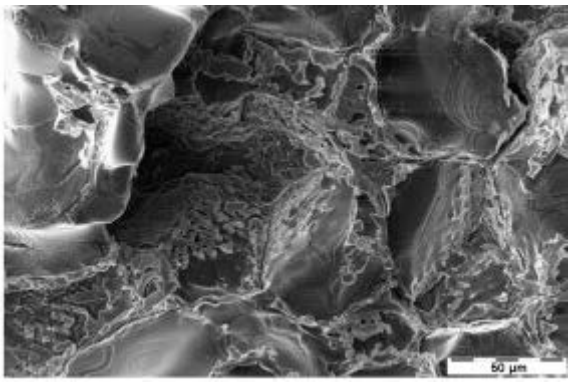

Figure 2.8 SEM image of magnesium alloy ZE41 tested in distilled water at ambient temperature (Bobby et al., 2008)

2.4.7 Stress Corrosion Cracking (SCC)

Metals under continued tensile stress in a specific corrosive environment can develop stress corrosion cracking (SCC). In this type of corrosion, the metal does not seem to be

under attack on most of its surface. However, fine cracks progress through the material due to tensile stress. These cracks spread deeper with time and can cause an unpredictable failure below the yield stress. To avoid stress corrosion cracking, cathodic protection is a suitable mitigation measure; however, it can immediately accelerate the hydrogen-embrittlement effect, which causes another kind of damage to the metal. The morphology of stress corrosion cracking appears as a brittle mechanical fracture but is actually the result of a local corrosion process. Stress corrosion cracking is proportional to time, increasing the stress decreases the time-to-failure of the metal. Factors such as temperature, electrolyte composition, metal chemical composition, stress and the structure of the component influence stress corrosion cracking. Figure 2.9 shows stress corrosion cracking in friction stir welded (FSW) AZ31 Mg alloy.

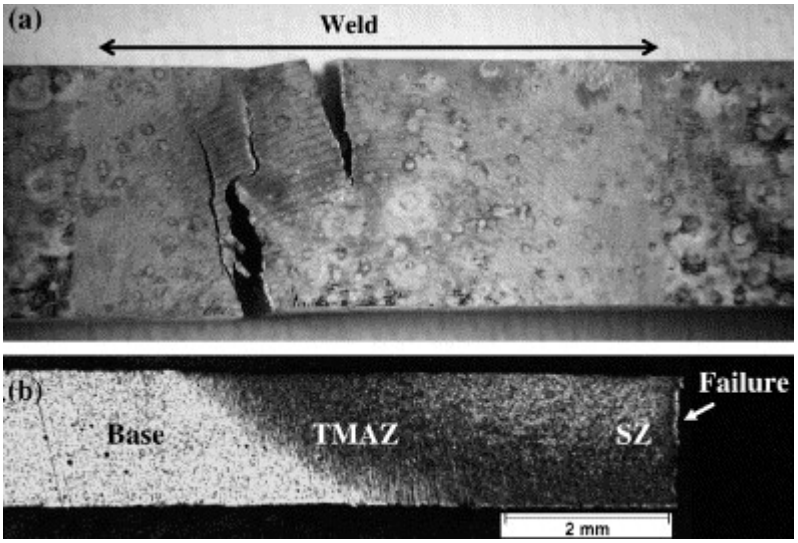

Figure 2.9 Stress corrosion cracking: corrosion of friction stir welded AZ31 Mg alloy tested with the slow strain rate tensile test method. In figure (b) SZ & TMAZ represents the Stir Zone and Thermos Mechanically Affected Zone respectively (Kannan et al., 2007)

2.5 Conducting Polymers

Conducting polymers are designed to carry electric charge. The important and well-known role of conductive polymers used as corrosion inhibitors is to protect metals, and they are produced either by chemical or electrochemical synthesis. Conductive polymer coatings have received great importance due to their high conductivity, easy processing, economic viability and environmental sustainability (Ewa, 2011; Gospodinova et al., 1998). The mechanism of the corrosion protection of metals by conducting polymers occurs in two stages: the first is the establishment of a thin passive layer and the second is the forming of a physical barrier (coating formation) (Camalet et al., 2000; Hongbin et al., 2011). The conductive properties make polymer coating materials ideal candidates for metal protection. However, the coating deposition typically depends on the concentration of the acid-polymer ratio, oxidation rate and oxidant, pH and temperature of the solution (Sayyah et al., 2016; Sapurina et al., 2012)

Polymers such as polyaniline polypyrrole and polythiophene are conducting polymers that are useful for corrosion protection. However, the mechanism of polymerisation of polyaniline in terms of oxidation is different from the polymerisation mechanism of other polymers. Polyaniline is characterised as a three-stage oxidation conducting polymer. During the polymerisation process, propagation occurs as leucoemeraldine, emeraldine and perningraniline oxidation states. In the polyaniline coating mechanism, a nitrogen atom is not only involved in the formation of a radical cation, but also plays a role in the conjugation of a double bond system. (Fatemeh, 2006; Toshiaki, 2012). There are many types of conducting polymers used in corrosion protection such as polyline, polypyrrole, polythiophene as it can be seen in figure 2.10. Figure 2.11 illustrates the mechanism of the polymerisation of aniline.

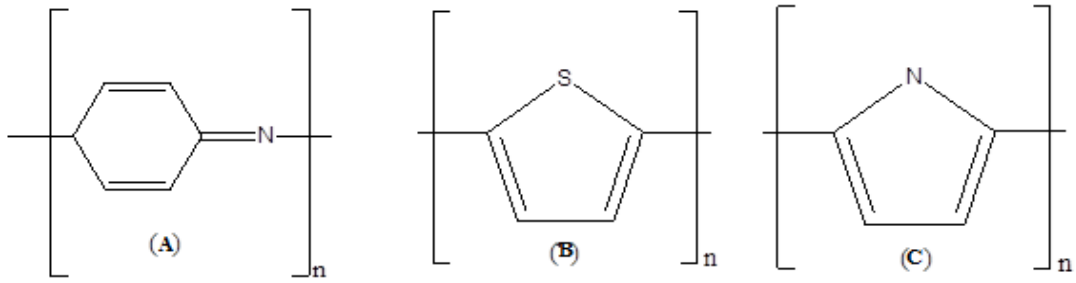

Figure 2.10 Typical conducting polymers: (A Polyaniline (PAni); (B) Polythiophene (PThio); and (C) Polypyrrole (PPy) (Toshiaki, 2012)

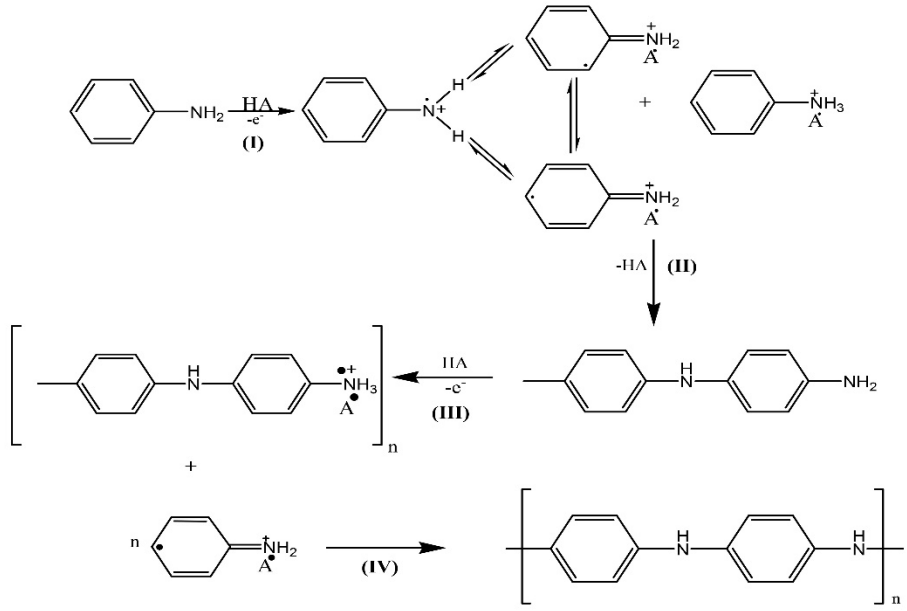

Figure 2.11 Electropolymerisation mechanism of aniline to polyaniline (Gvozdenovic et al., 2011)

2.5.1 Polyaniline

Polyaniline (PANI) can be prepared by chemical or electrochemical oxidative polymerisation with a conductivity range of 10^{-1}–10^{1} S.cm^{-1} depending on factors such as ionic and proton conductivity and redox kinetics. Polyaniline can be prepared in three distinct oxidation-state conductive polymers. These oxidation stages are known as,

1. Leuoemeraldine. This state of oxidation is described as the fully reduced form of the oxidation of a leucoemeraldine base.

2. Emeraldine. This is the state of the reaction of an emeraldine base in which a half oxidation reaction takes place.
3. Perningraniline. This state is the fully oxidized form of polyaniline.

Emeraldine is the oxidated state of polyaniline and forms a dark green-coloured coating with a higher degree of conductivity. The three different oxidation states are categorised according to changes in colour. For instance, the leucoemeraldine oxidation state is transparent and colourless, emeraldine salt is green and emeraldine base is blue; whereas pernigraniline has a blue/violet colour. Of the three distinct oxidation states, the emeraldine salt has the highest conductivity. Emeraldine is neutral like all other oxidated forms of aniline and, if doped (protonated), it changes to emeraldine salt, with the amine nitrogens protonated by an acid. During the reaction, imines are responsible for protonation (transfer of protons) to form bipolarone emeraldine salt. Compared to leucoemeraldine and pernigraniline, emeraldine as a form of polyaniline is highly stable at room temperature during chemical and electrochemical reactions. The electrical conductivity of this distinct form of polyaniline varies in most cases. However, the emeraldine base, if doped with acid, increases the conductivity by ten orders of magnitude (Fatemha, 2006; Jeroslav et al., 2010; Milica, 2009). Figure 2.13 shows the three different oxidations states of the polymerisation of aniline.

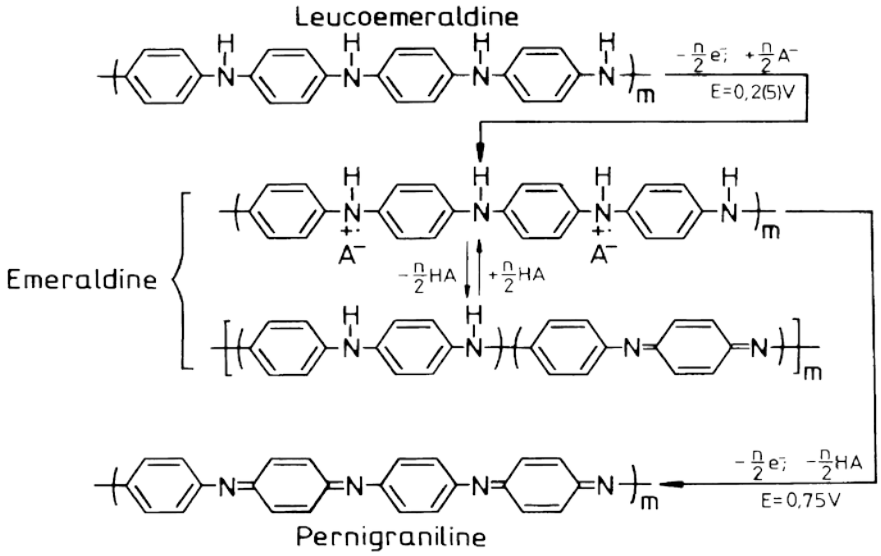

Figure 2.12 Electropolymerisation mechanism of three oxidation states of aniline (Gospodinova & Terlemezyan, 1998)

Zhang et al. (2013) chemically coated AZ91D magnesium alloy with a polyaniline/organophilic montmorillonite epoxy coating to enhance its corrosion resistance. The performance of the coating was tested by immersion for 6000 h in a 3.5% NaCl solution. The results showed that the organophilic montmorillonite coating acted as a physical barrier and the PANI coating created an oxide layer on the magnesium alloy. The formation of a PANI passive layer is mainly attributed to the emeraldine base salt of aniline, which is one of the oxidation states of PANI.

2.5.2 Polypyrrole

Polypyrrole is a common conducting polymer used in commercial applications for biosensors, gas sensors, wires, microactuators, antielectrostatic coatings, capacitors, polymeric batteries and electronic devices. The synthesis of polypyrrole can be done chemically or electrochemically. The thickness and formation of polypyrrole film depend upon factors such as the monomer to dimer and dimer to polymer oxidation of the

electrolyte bath, and the polymerising temperature, pH and kinetics of the coating procedure.

Kaplin and Qutubuddin (1995) reported that involvement of electrons and ion transport in an electrical conducting polymer during a redox reaction changes the electrical properties of a film from that of an insulator to being an electrically-conductive polymer film on a glassy carbon electrode. Singh et al. (2004) reported that, generally, a coating film can be obtained through electrodeposition techniques such as cyclic voltammetry, galvanostatic and potentiostatic techniques. However, in most cases, electropolymerisation is carried out on noble metals due to the fact that the standard oxidation potential of pyrrole is high (E_{ox} = 0.70V vs SCE). In the case of coating reactive metals, dissolution of most of the metal takes place prior to the oxidation of the monomer and, thus, the electropolymerisation reaction is inhibited.

Lin-Xia et al., (2001) reported that polypyrrole can form a blend with insulating polymers more easily than polyaniline and polythiophene, whereas polyaniline can deposit onto reinforcing textiles and polyalkylthiophene has excellent solubility and melting characteristics. Polypyrrole also has good conductivity and better environmental stability. However, the mechanical property of the polymer is poor.

2.5.3 Polythiophene

Polythiophene is considered a good conducting polymer, not only due to its excellent thermal stability and good conductivity, but also for its high transparency in the visible light range. The synthesis of the polymer can be done by either chemical or electrochemical methods. The electrodeposition of polythiophene can be done by cyclic voltammetry, galvanostatic and potentiostatic techniques. However, coating formation

can be affected by factors such as current density, the polymerisation agent/solvent used, the concentration of the polymer, temperature, time and coating conditions.

Batteries, fuel cells, corrosion protection and chemical sensing are some of the examples of polythiophene applications. Abou-Elenien et al. (2004) reported that electropolymerisation of polythiophene coating on a platinum disk can be achieved by galvanostatic, potentiostatic, potentiodynamic and chronoamperometric techniques. The solvents used were dichloromethane (DCM), 1,2-dichloroethane (DCE), acetonitrile (AN), and nitrobenzene (NB). The supporting electrolytes were lithium perchlorate ($LiC1O_4$), tetraethylammonium perchlorate ($TEAC1O_4$), tetrabutylammonium perchlorate ($TBAClO_4$) or tetrabutylammonium hexafluorophosphate ($TBAPF_6$). The results revealed that the most stable polythiophene coating was achieved with an electrolyte bath of AN used as a solvent, with a supporting electrolyte of tetrabutylammonium hexafluorophosphate ($TBAPF_6$) with bithiophene 0.01 M at 5 °C, via the galvanostatic technique. The coating measurements of the film obtained by polythiophene were calculated according to coating time under different conditions. Various factors such as electrolyte composition, temperature and current applied affect the thickness of the film.

2.6 Electropolymerisation

In recent years, electrochemical polymerisation techniques have been widely used due to their characteristics of being environmental friendly, easy to process, rapid and requiring few chemical additives. The performance of conducting polymers has two components: the effect of the polymer coating layer, and the chemical reaction at the metal-polymer interface (Breslin et al., 2005; Vered et al., 2001). The synthesis of polymer coatings is a challenge when forming coatings on active metals, due to oxidation or prior dissolution

of the metal substrate. Oxidation reaction peaks during cyclic voltammetry have been observed due to metal dissolution (Kang et al., 2009). Thus, dissolution is an obstacle to forming an adherent coating at the metal surface. Many researchers have used mineral acids such as sodium sulphate (Na_2SO_4), sulphuric acid (H_2SO_4), hydrochloric acid (HCl), and nitric acid (HNO_3) as oxidizing/doping agents (Borole et al., 2006; Ocon et al., 2005; Sauza et al., 2007). However, these mineral acids have been replaced by oxalic acid and sodium salicylate in several studies due to the fact that these supporting agents have fewer dissolution effects on the substrate (Kang et al., 2009; Kazum et al., 2013; Martyak et al., 2002).

Polyaniline and polypyrrole are extensively studied conducting polymers used for corrosion protection of metals (Benyaich et al., 1996; Biallozor et al., 2005; Gospodinova et al., 1998), such as low carbon steel (Raotole et al., 2013), stainless steel (Heydari et al., 2016; Sazou et al., 2007), carbon substrates (Dalmolin et al., 2005), mild steel (Ocan et al., 2005; Pawar et al., 2006), copper (Cascalheira et al., 2003), aluminium (Gvozdenovi et al., 2009; Martins et al., 2008) and magnesium (Rong-Gang et al., 2012; Sathiyanarayanan et al., 2006). Polyaniline has been studied as an effective polymer coating to enhance the corrosion resistance of most metals and as a coating for different metals with different polymerising agents and chemical/electrochemical techniques (Lao et al., 2015; Rout et al., 2003; Radhakrishnan et al., 2009; Sambyal et al., 2016).

The polymerisation of aniline has been investigated with several polymerisation agents such as sodium salicylate (Kazum et al., 2013), sulphuric acid (Sazou et al., 2007; Dalmolin et al., 2005), oxalic acid (Heydari et al., 2016) and sodium benzoate (Gvozdenovi et al., 2009).

The synthesis of these polymers has demonstrated protection of the metal surface by passivation during redox characteristics of the polymerization (Cascalheria et al., 2008; Gvozdenovi et al., 2009; Pawar et al., 2006). However, the passive films in reactive metals such as magnesium and its alloys are not stable compared to those of other metals such as aluminium, copper, zinc and steel (Nobuyoshi et al., 2007). The deposition of the coating depends upon parameters such as coating technique (Arenas et al., 2008; Kazum et al., 2013; Ling et al., 2008; Pawar et al., 2006), the kinetics of the coating process (Gospodinova et al., 1998; Gvozdenovic et al., 2011), and the metallic substrate to be coated low carbon steel (Raotole et al., 2013), stainless steel (Sazou et al., 2007; Heydari et al., 2016), carbon substrates (Dalmolin et al., 2005), mild steel (Ocan et al., 2005; Pawar et al., 2006), copper (Cascalheira et al., 2003), aluminium (Martins et al., 2008; Gvozdenovi et al., 2009) and magnesium (Rong-Gang et al., 2012; Sathiyanarayanan et al., 2006).

2.7 Electropolymerisation techniques

Conducting polymers can be synthesised either by chemical or electrochemical methods. Electrochemical techniques are environmentally sustainable, cheap, easy to process and, hence, are promising. A few electrochemical techniques have been used to form adhesive polymer coatings on various metals. The common methods are potentiostatic, galvanostatic and cyclic voltammetry techniques (Ocon et al., 2005; Fang et al., 2007; Sazou et al 2007).

2.7.1 Galvanostatic Technique

The galvanostatic or constant current technique has been used to produce polymer coatings that enhance the corrosion protection of low carbon steel (Iroh et al., 2000). A coating electrolyte of polypyrrole and oxalic acid was used to apply a 0.5 mm-thick

coating on low carbon steel at 0.56 mA/cm^2 constant current density. Table 2.3 shows the potentiodynamic polarisation response of the corrosion resistance at different pH scales. Polypyrrole and poly(N-methylpyrrole) coating was applied to low carbon steel at a pH range of 1.4 to 4.1. The results revealed that the polypyrrole coating applied at pH 2.4 achieved better corrosion protection than that at pH 1.4 and 4.1 (in 1 M NaCl solution). The lowest corrosion rate of 0.004 mm/yr was achieved at pH 2.4. The authors described the coating process in three stages: passivation, decomposition and polymerisation.

Table 2.3 DC polarisation results of the coating effect of polypyrrole and poly(N-methylpyrrole) coatings applied at different pHs in 1 M NaCl (Iroh et al., 2000)

Sample	**Ecorr (mV)**	**Icorr (A/cm^2)**	**Corrosion rate (mm/yr)**
Bare steel	-601	9.1E-05	1.05
FeC_2O_4- $2H_2O$ pH 1.4	-699	1.4E-04	1.67
FeC_2O_4- $2H_2O$ pH 2.4	-692	1.2E-04	1.40
Polypyrrole, pH 1.4	-102	5.5E-06	0.06
Polypyrrole, pH 2.4	-16	3.6E-07	0.004
Polypyrrole, pH 4.1	-186	3.1E06	0.04
Polymethylpyrrole			
(i) pH 1.4	-430	4.3E-06	0.05
(ii) pH 2.7	-580	6.4E06	0.07

O'Kazum et al. (2013) used electrolyte containing 0.3 M aniline with 0.1 M sodium salicylate to coat polyaniline on steel at different current densities under stirred and non-stirred bath conditions (Figure 2.13). The stirred bath condition was used to reduce bubble formation during current application; however, the study suggests that the sample coated at 20 mA cm^{-2} in a stirred bath had better corrosion resistance than that at 25 mA cm^{-2}. At higher current densities, bubble formation was high and hindered the formation of the coating.

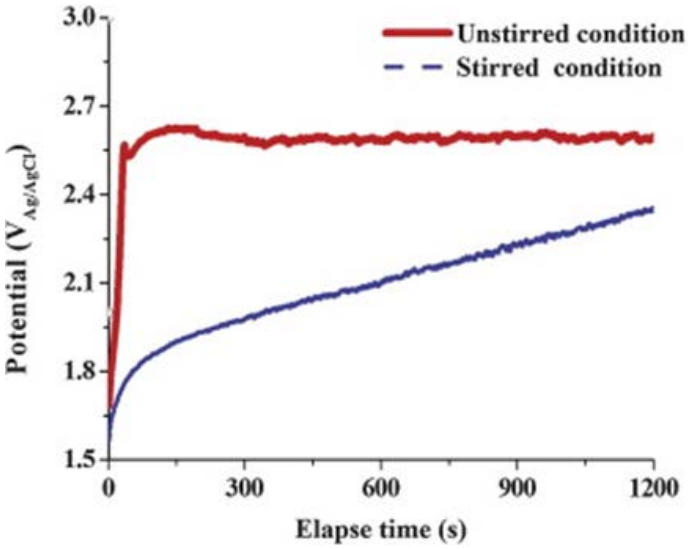

Figure 2.13 Galvanostatic curves of polyaniline coating of steel under unstirred and stirred electrolyte bath conditions (O'Kazum et al., 2013)

Bakkar et al. (2007) used various ionic liquids to electrodeposit Zn on magnesium alloy by cyclic voltammetry and constant and pulse galvanostatic techniques (Figure 2.14). The authors studied the electrodeposition of Zn using ionic-based choline chloride/ethylene glycol ($HOCH_2CH_2OH$) (ChCl/EG) by constant current densities of 2.5, 5 and 10 mA/cm^2. The study suggests that at both low and high current densities, the Zn coating layer was porous. However, the coating layer formed at 5 mA/cm^2 was denser than that formed at 2.5 and 10 mA/cm^2. The authors also suggested that during pulse galvanostatic coating between -5 mA/cm ^{2} to 0.0 mA/cm^2 with a looped 2 seconds on -1 second off pulsed current, the nucleation rate of the coating was increased and the coating layer obtained was smoother and without pores, compared to coatings at constant current densities.

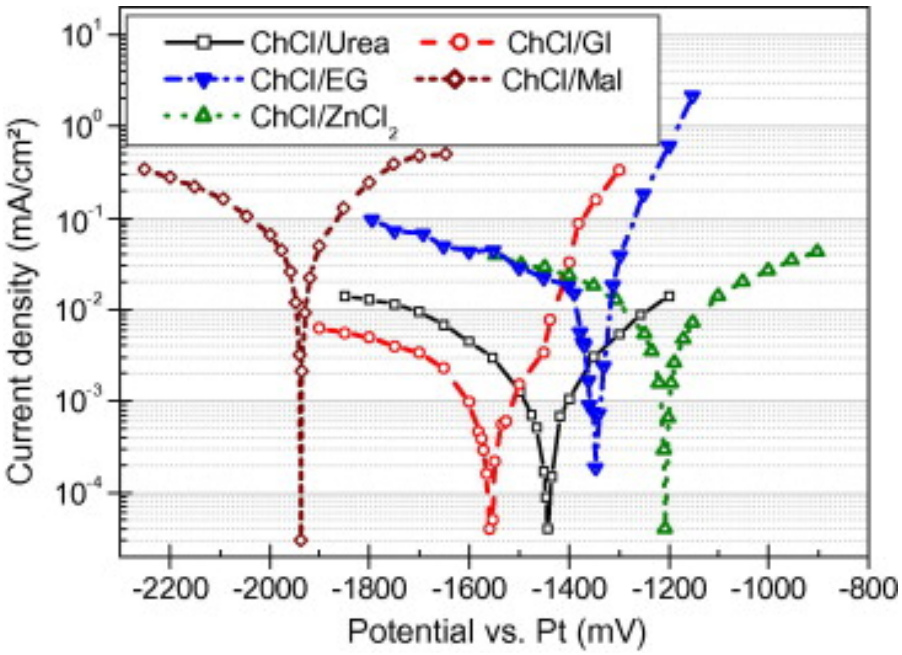

Figure 2.14 Potentiodynamic polarisation curves of Cp Mg in different ionic liquids at 60 °C (Bakkar et al., 2007)

Ezhilselvi et al. (2016) produced Micro-arc oxidation (MAO) coating on AZ31B magnesium alloy at constant current densities of 0.026, 0.046 and 0.067 A/cm^2 (Figure 2.15) in an alkaline solution at pH 11. The coating obtained at low current density (0.026 A/cm^2) appeared to be relatively uniform and more porous than those obtained at high current density (0.067 A/cm^2). The porosity of the coating decreased as the current density increased; and at the same time, the diameter of the pores increased. The potentiodynamic polarisation tests in 3.5% NaCl solution suggested that the coating obtained at 0.046 A/cm^2 had a corrosion current of 7.79 × 10^{-10} A/cm^2, which is lower than that obtained at 0.026 and 0.067 A/cm^2.

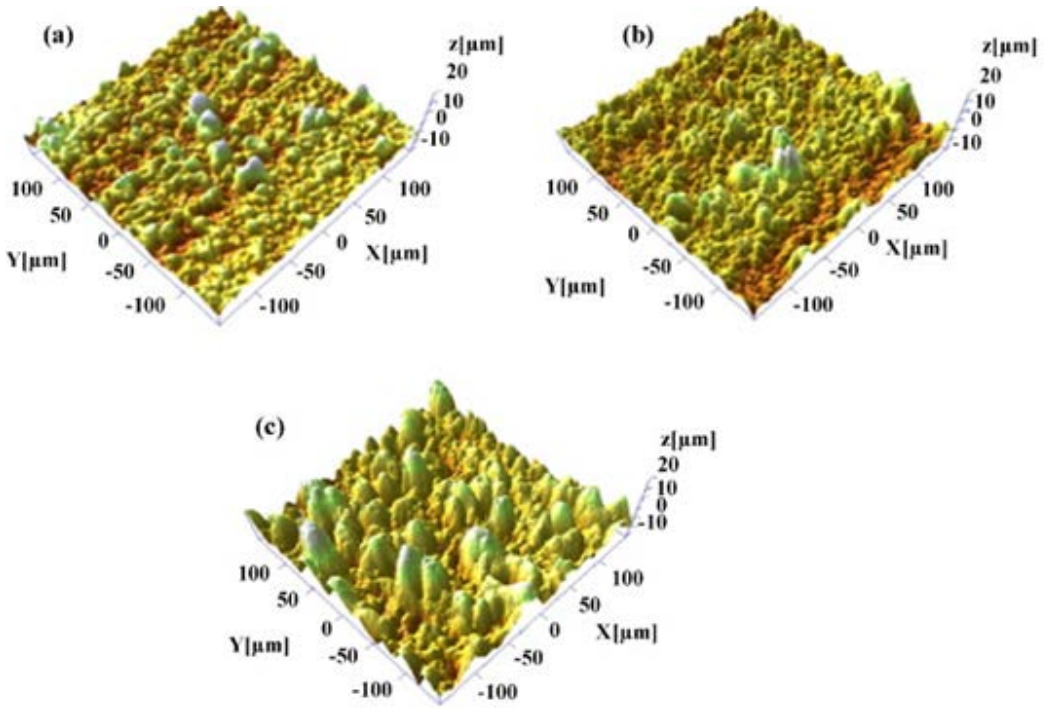

Figure 2.15 3D topographical images of MAO coatings prepared at different current densities: (a) 0.026 A/cm^2, (b) 0.046 A/cm^2 and (c) 0.067 A/cm^2 coatings, respectively (Ezhilselvi et al., 2016)

2.7.2 Potentiostatic technique

The potentiostatic technique has been used by several researchers to form polymer coatings on various metals. Wang and Tan (2006) used aluminium AA1100 (wire beam electrode, WBE) to form polyaniline (APNI) coating with an electrolyte of 1 M tosylic acid and 0.16 M aniline. The coating was produced at a constant potential of 1.25V vs saturated calomel electrode (SCE). The study suggests that the aluminium electrode undergoes passivation during the PANI polymerisation process. Furthermore, the wire beam electrode (WEB) anodic current decreased from 0.321 mA/cm^2 to 0.168 mA/cm^2 due to the electrode's exposure to the PANI solution. The reduction in the anodic current is due to the barrier between the electrolyte and the metal, which shows the formation of polyaniline deposition (Figure 2.16). During a potentiodynamic test in 0.5 M NaCl solution, the PANI film ennobled the E_{pit} of the aluminium electrode AA1100 for about

130 mV. The coating was non-uniform, which could lead to general corrosion of the AA1100 aluminium electrode.

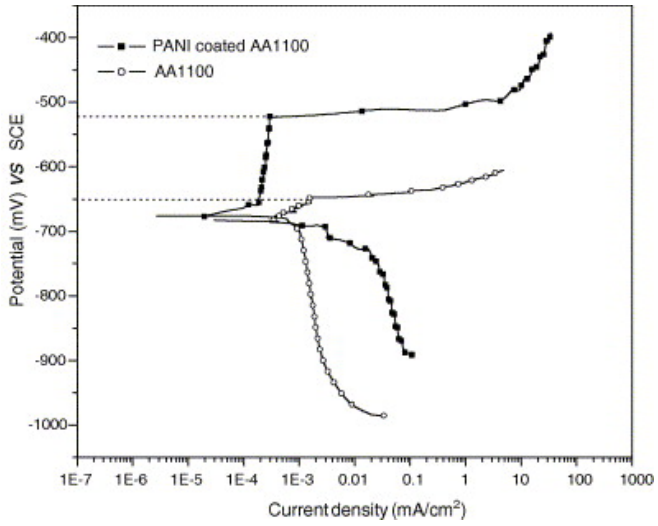

Figure 2.16 Potentiodynamic polarisation curves of PANI-coated AA1100 and bare AA1100 in 0.5 M NaCl solution (Wang and Tan, 2006)

2.7.3 Cyclic voltammetry technique

Cyclic voltammetry is an electrochemical technique that has been used by several researchers. In this technique, the working electrode potential is ramped-up linearly over time. Cyclic voltammetry is performed by cycling the potential of the working electrode and measuring the resulting current.

Babaiee et al. (2015) used a 0.75 M HNO_3 and 0.25 M H_2SO_4 solution to electropolymerise 0.1 M aniline at a graphite electrode (Figure 2.17). Two electrodeposition conditions were tested at room temperature using the cyclic voltammetry technique. During the first condition, the sweep rate was –0.2 and 1 V vs Ag/AgCl with different scan rates of 12.5, 25, 50, 75 and 100 mV s^{-1}. However, for the second polymerisation condition, the potential was scanned in the range of –0.2 to 0.9, 1 and 1.1 V at a scan rate of 25 mV s^{-1}. During the electrodeposition tests with various potentials and scan rates, the optimised current density was achieved at a potential of –

0.2 to 1 V. Electrodeposition of aniline (oxidation of PANI) only occurred with the potential range of 0.9–1.1 V. However, from −0.2–0.9 V, the electrodeposited PANI underwent reversible redox reactions.

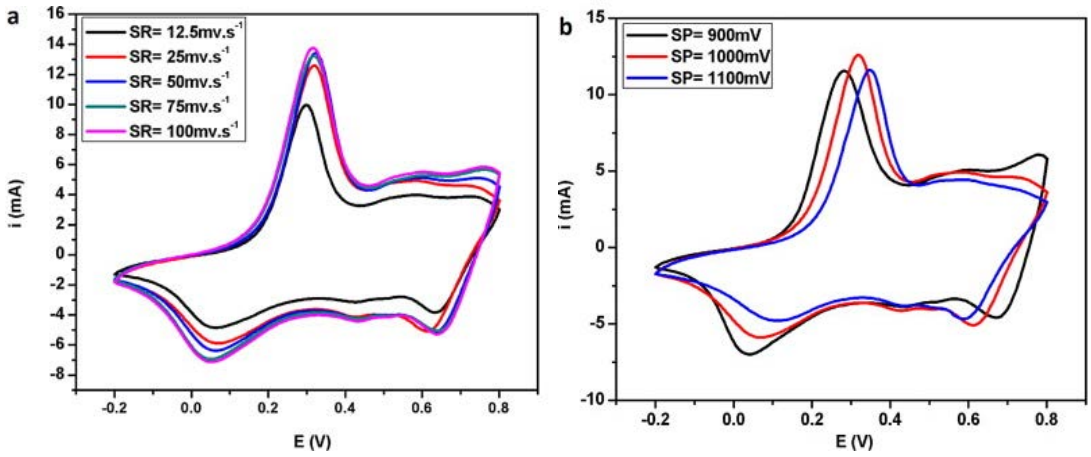

Figure 2.17 Cyclic voltammetry test on polyaniline, performed under different electropolymerisation conditions: (a) effect of different scan rates, (b) effect of different switching potentials (Babaiee et al., 2015)

Rovshan et al. (2009) used a 0.3 M oxalic acid and 0.1 M aniline coating bath to electropolymerise a PANI coating on a steel substrate using the cyclic voltammetry technique (Figure 2.18). It can be seen that the initiation of the first monomer radical cation occurred at +1000 mV during the first cycle. However, due to continued growth of PANI, the potential got reduced to +400 and +350 mV during the second and the third cycles, respectively. During the backward scan, repassivation was observed at +90 mV. Hence, the potential of the backward scan for passivation dropped to +70 and +50 mV for the second and third cycles, respectively. The study used immersion tests to show that PPY/PANI and PANI/PPY coatings exhibited 86.8% better inhibition efficiency in 1 M H_2SO_4 compared to that of bare metal.

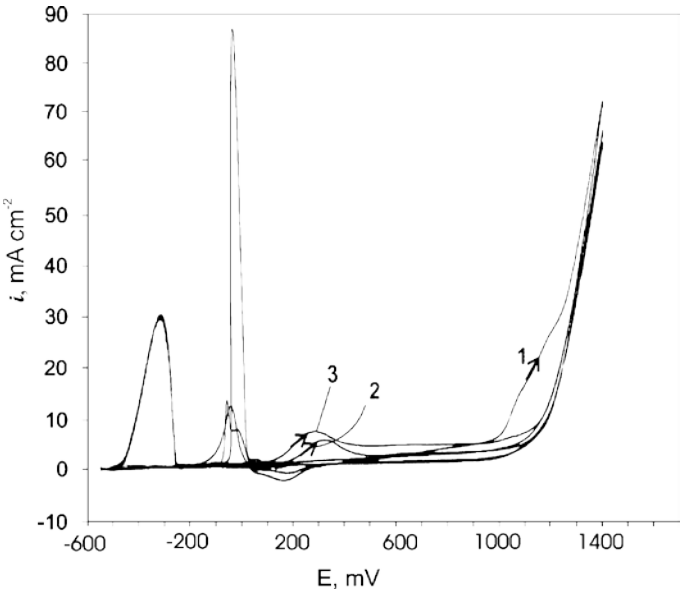

Figure 2.18 The initial three cycles of voltammogram for the electrochemical synthesis of PANI (0.1 M aniline and 0.3 M oxalic acid) solution coating on steel (Rovshan et al., 2009)

2.8 Effect of electrolyte pH

Polymerisation of aniline is generally dependent on selection of electrolyte parameters. The pH of the coating bath is critical, due to fact that the ideal pH for the synthesis of the aniline is acidic (Fatemah 2006). Magnesium alloys are reactive metals and it is challenging to form a protective polymer coating on them in an acidic electrolyte. In high pH polymer electrolytes, it is also difficult to form polymer coatings on magnesium alloys. Mostly strong acids, as oxidants, are ideal to incorporate into polyaniline synthesis to form conductive coatings, which can only take place at low pH. At low pH values < 2.5, highly conductive polyaniline with a high molecular weight and well-developed polyconjuction system is obtained. However, at high pHs, there is low conductivity and no polyconjuction polyaniline oligomers (Yu et al., 2012).

Low protonation of aniline, *p*-aminodiphenylamine at $pH_{(synth)}$ 11 has been reported. It was suggested that the conductivity of the polymer is low in a high pH, due to the fact that the potential is not high enough at the polymer/solution interface (Xiao-Xia et al.,

2005). Further, Gospodinova et al., 1998 suggested that the oxidation potential of the polymer chain decreased with increasing pH. A high pH electrolyte apparently slows the redox process and lowers the oxidation potential of the polymerisation process. The potential decreases significantly on deprotonation of the polymer chain. Aniline oxidation takes place at different pH levels and forms different molecular structures, morphologies and properties. Oxidation takes place due to the presence of a monomer and growing chain in protonated and deprotonated formation, which possess different oxidation potentials.

2.9 Effect of coating time

Coating time is a vital factor that affects the structure, hardness, thickness and morphology of coatings obtained by electrodeposition. Sorkhabi et al. (2004) chemically coated mild steel in nickel-phosphorus alloy from a bath containing sodium hypophosphite and glycin-citrate complexing agents. The coatings obtained at 0.5 and 3 hours were tested in 3.5% NaCl solution by potentiodynamic polarisation tests. Figure 2.19 shows that the corrosion potential (e_{corr}) was significantly shifted in the active direction. The results show that the 3-hour coating time considerably affected the coating performance of the nickel-phosphorus alloy coating.

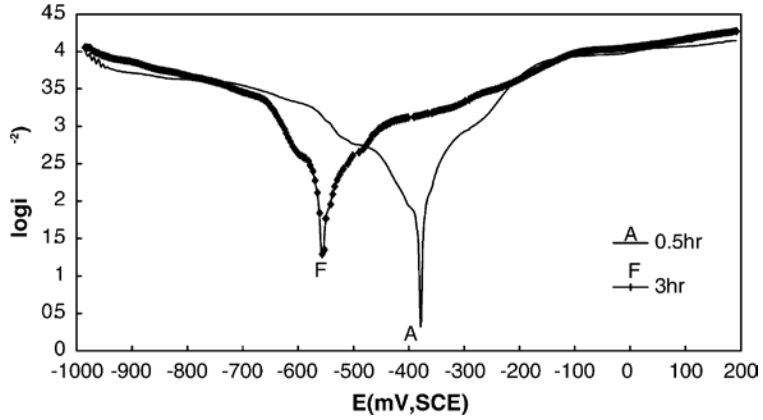

Figure 2.19 Polarisation curves of as-plated nickel-phosphorus alloy deposited from a bath containing sodium hypophosphite and glycin-citrate complexing agents and tested in 3.5% NaCl solution (Sorkhabi et al., 2004)

Yantapure et al. (2015) coated low carbon steel in a zinc phosphating bath containing zinc oxide. Current densities of 2, 4, 6, 8 and 10 mA/cm^2 were used to form coatings on a metal substrate for durations of 20, 40 and 60 minutes. The coating obtained at 4 mA/cm^2 current density had the lowest corrosion rate. In Table 2.4, the potentiodynamic polarisation results reveal that the shift of anodic potential was –408 mV at 4 mA/cm^2.

Table 2.4 Corrosion current density, corrosion potential and corrosion rates of bare steel and phosphated steel in 3.5% NaCl solution (Yantapure et al., 2015)

Sample No.	Deposition current density (mA/cm^2)	Icorr (A/cm^2)	Ecorr (mV)	Corrosion rate (myp)
Uncoated	-	81.3	-697	9.19
Phosphate coated	2	78.40	-548	4.48
Phosphate coated	4	40.90	-408	2.33
Phosphate coated	6	83.90	-537	4.79
Phosphate coated	8	87.40	-542	4.99
Phosphate coated	10	94.30	-530	5.38

Table 2.5 shows the Electrochemical Impedance Spectroscopy (EIS) results of coating deposition time. Increased coating deposition time significantly increased the coating

thickness. Coating thickness decreased the porosity and this resulted in a decrease in coating capacitance.

Polymer chain growth at low pHs is significant. However, if the potential or the current (potentiostatic or galvanostatic) of the electrochemical reaction is high, the polymer coating can be achieved even faster. Hence, if the metal which needs to be coated is reactive, then a higher potential/current can lead to dissolution of the metal (Kirkland et al., 2012).

Table 2.5 EIS results for zinc phosphate-coated steel samples at 4 mA/cm^2 for 20, 40 and 60 min in 3.5% NaCl solution (Yantapure et al., 2015)

Deposition time (min)	Current density (mA/cm^2)	Coating resistance R_c(Ω.cm^2)	Coating capacitance C_c (F)	Warburg constant W_d	Z_{mod} (Ω.cm^2)	Z_{real} (Ω.cm^2)
20	4	184	0.40	274.69	152.7	90.63
40	4	255.5	0.33	212.44	202.7	128.5
60	4	406.8	0.20	11.01	328.8	214.1

Table 2.6 Summary of the literature on alloy corrosion prevention using conducting polymers

Material	Coating	Test method	Observation	Reference
Steel plates	Polyaniline-nano-TiO2	Potentiodynamic polarisation in 3.5% NaCl solution	Nano-TiO_2 improved the PANI performance by improvement of barrier properties, redox behaviour of PANI and formation of p-n junctions	Radhakrishnan et al., 2009
Mild Steel	Poly(aniline-co-phenetidine)/SiO2	Potentiodynamic polarisation in 3.5% NaCl solution	As per ASTM B117, no extended corrosion or blistering along the scribe mark	Sambyal et al., 2016
Steel	PANI	Potentiodynamic polarisation in 3.5% NaCl	Enhanced corrosion resistance in stirred conditions	Kazum et al., 2013
AA100 Alloy	Polyaniline coating	Potentiodynamic polarisation in 0.5 % NaCl solution	Coating enhanced corrosion resistance but coating also showed irregular pores with cracked morphology	Ezhilselvi et al., 2016
Steel	Bilayer PPY/PANI, PANI/PPY coatings	Potentiodynamic polarisation in 1 M H_2SO_4	PPY/PANI coatings offered superior corrosion protection compared to PANI/PPY coatings	Hasanov et al., 2009
Carbon substrate	Polyaniline coating	EIS in 0.5 mol L^{-1} H_2SO_4 aqueous solution.	Coating morphology was improved	Dalmolin et al., 2005
Copper	Polypyrrole	Galvanostatic and potentiostatic methods. Coating tested by adhesion	Pore-free uniform coating obtained. Potentiostatic tests showed poor adhesion	Cascalheria et al 2003
Aluminium alloy 6061-T6	Polypyrrole	Anodic polarisation in 0.5 M NaCl solution	Coating could not protect the material as the value of the corrosion and the pitting potential remained unchanged	Matins et al., 2008
430 SS	Bilayer of poly(3-aminobenzoic acid), polyaniline	Potentiodynamic polarisation in 3.5% NaCl solution	Bi-layer PABA(10)/PANI (10) coating performed well compared to mono-layer PABA and PANI coatings	Heydari et al., 2016
Low carbon steel	Polypyrrole	SEM/optical evaluation	Uniform and strongly adherent PPY coating on LCS was formed	Raotole et al., 2013

Table 2.7 Summary of the literature on corrosion prevention by using different coatings on magnesium alloy

Material	Coating	Test method	Observation	Reference
AZ91 magnesium alloy	Polyaniline/organophilic montmorillonite epoxy	Immersion in 3.5% NaCl	Corrosion protection of PANI film reduced in presence of O_2	Zhang. et.al., 2013
AZ31 alloy	6-dihexylamino-1,3,5-triazine-2,4-dithiol monosodium (DHN)	Potentiodynamic polarisation in 3.5% NaCl	i_{corr} enhanced from 8.43 μA/cm^2 to 0.78 μA/cm^2	Kang. et al., 2009
ZM 21 alloy	Acrylic-polyaniline	EIS in 0.5 % NaCl	Anticorrosion coating resistance was increased	Sathiyanarayanan et al., 2006
AZ91 magnesium alloy	Anodised alkaline silicate	EIS in 3.5 % NaCl	Protection enhanced	Ling et al., 2008
Magnesium alloy	Zn coating	Potentiodynamic polarisation in 0.1 M NaCl solution	Corrosion resistance decreased due to micro cracks in the coating	Bakkar et al., 2007
AZ31B alloy	Alkaline Silicate (Na_2SiO_3 + NaOH + NaF) coating	Potentiodynamic polarisation in 3.5 % NaCl solution	Corrosion resistance increased coating also showed irregular pores with cracked morphology	Ezhilselvi et al., 2016
Magnesium alloy	Polyaniline in alkaline solution	SEM evaluation	Strongly adhesive coating was formed but was deeply dependent on electrochemical parameters	Guo et al., 2003
AZ91D	Polyaniline	Salt spray/SEM evaluation	Polyaniline/epoxy coating significantly enhanced corrosion resistance of Mg alloy	Luo et al., 2015

CHAPTER 3 Materials and Experimental Procedure

This chapter details the alloy and electropolymerisation and characterisation techniques used in this work.

3.1 Material

The AZ91 magnesium alloy was used as a base metal for coating. The chemical composition of the alloy is given in Table 3.1. Samples (size: 20 mm × 20 mm × 2 mm) were initially ground with SiC paper (up to 2500 grit) followed by ultrasonic cleaning in acetone.

Table 3.1 Chemical composition of the magnesium alloy used in this study.

Al	Zn	Mn	Fe	Cu	Si	Mg
8.81	0.79	0.21	0.003	0.003	<0.01	bal

3.2 Electropolymerisation

Electropolymerisation was carried out using a potentiostat (VersaSTAT 3 PAR) and a typical three-electrode cell. The cell used an alloy sample as the working electrode, silver/silver-chloride (Ag/AgCl) as the reference electrode and graphite as the counter electrode.

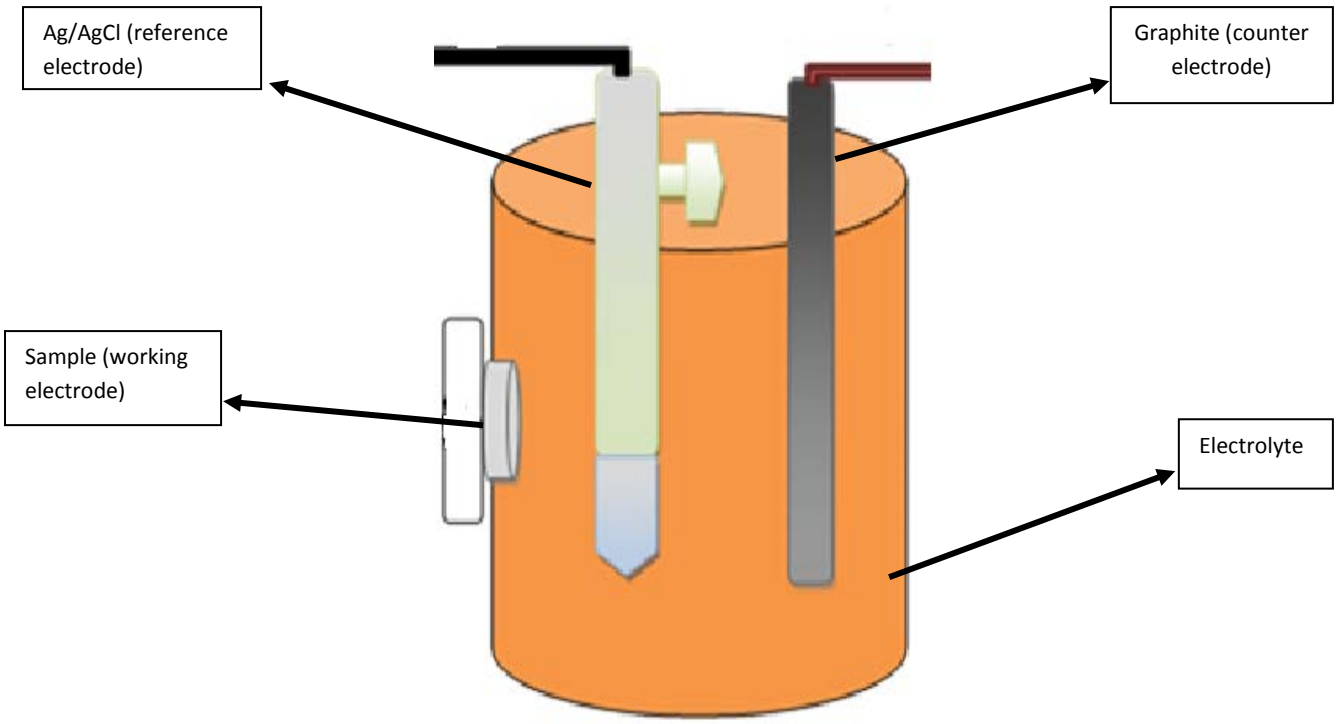

Figure 3.1. Schematic image of the three-electrode cell used for electrochemical experiments

3.2.1 Cyclic voltammetry method

Cyclic voltammetry is a polarisation technique used for electrochemical measurements. In this technique, the set potentials are applied in a number of cycles to measure the current in a three-electrode cell. The potential is measured between the working electrode and the reference electrode, while the current is measured between the reference and counter electrodes. During polarisation testing at the selected potential, the anodic and cathodic currents are measured in forward and reverse scans. The cyclic voltammetry tests depend up the number of the cycles and selected scan rate.

A cyclic voltammetry technique (parameters: cycles = 5; vertex 1 and 2 potentials of -1 V and 2.2 V, respectively) was used for electropolymerisation of aniline. Two different electrolytes were used for the coating: 0.3 M aniline + 0.1 M sodium salicylate ($C_7H_5NaO_3$), and 0.2 M aniline + 0.25 M potassium hydroxide (KOH). The coatings produced from these two electrolytes will hereafter be called the PASS and PAPH coatings, respectively. After electropolymerisation, the coated samples were placed in an oven at 80 °C for 24 h to remove any residual electrolyte.

Pre-treatment of the alloy prior to polymer coating on the surface of AZ91 magnesium alloy samples was conducted in 3 M sodium hydroxide solution. The pre-treatment was an attempt to enhance the coating formation and passivation, thereby increasing corrosion resistance. The passivation of the alloy was done at two different constant potentials: -750 and -195 mV. For the polyaniline coating, the number of cycles for the pretreated samples was 15.

3.2.2 Galvanostatic method

Galvanostatic is an electrochemical technique referring to an experimental testing procedure in which a three-electrode cell is maintained at a constant current to observe electrochemical reactions. In this technique, a constant current is applied to understand the kinetics and mechanisms of the electrode reactions. In the galvanostatic technique, the current between the working and counter electrodes is controlled, and the potential between the working and reference electrodes is measured. This technique is suitable for commercial and industrial purposes due to its easy one-step operation.

In the present study, during galvanostatic coating, current densities of 14, 18 and 20 mA/cm^2 were selected for the electropolymerisation process. Coating was conducted for

600 seconds. For any after electropolymerisation, the coated samples were placed in an oven at 80 °C for 24 h to remove any residual electrolyte.

3.3 Coating Characterisation

Coatings were characterised by coating thickness tests, adhesion tests and chemical/molecular analyses before and after corrosion morphological analysis.

3.3.1 Microscopic analysis

Microscopic analysis was done to characterise the samples at the micro scale. The technique can be used for morphological analysis, mechanical failure and physical characterisation. An optical microscope (Nikon Eclipse 50i POL) was used to analyse the morphology of coatings before and after potentiodynamic polarisation tests. The microscope was also used to analyse the grinding and polishing of samples before coating.

3.3.2 Coating thickness

Coating thickness analysis is essential to understand the performance of the electrochemical deposition of the polymer coating on the surface of the material. Coating thicknesses were measured using a coating thickness gauge (Fisher Dualscope MP0R). Non-ferrous coating thickness measurements were conducted using the eddy current technique.

3.3.3 Coating adhesion

Coating adhesion tests were used to assess the bonding of coatings to the metal surfaces. Coating adhesion tests can be done by several methods, such as the cross-cut, scrape adhesion, and pull-off tests. After coating polyaniline on the surface of the AZ91

magnesium alloy by electrochemical deposition, the samples were tested for adhesion by the pull-off test method. Measurements of pull-off adhesion were performed by an adhesion tester (Elcometer 106).

3.3.4 Scanning electron microscopy

Scanning electron microscopy (SEM) is an advanced technique used to analyse samples at the micro/nano scales. During the analysis, an image of the surface of a sample is created with a focused beam of electrons. These electrons interact with the atoms present at the surface of the sample. The electron beam is scanned in a raster scan pattern, and the beam's position is combined with the detected signal to produce a micro/nano-scale image of the morphology of the sample. The morphologies of coatings before and after potentiodynamic polarisation tests were observed with a scanning electron microscope (Jeol JSM 541OLV).

3.3.5. Fourier-transform infrared spectroscopy

Fourier-transform infrared spectroscopy (FTIR) is a molecular test for any liquid, solid or powdery samples. The test can be used for both qualitative and quantitative analyses. This technique is based on an infrared light source: the light beam goes through the sample and the absorbance of light is analysed. Transmittance can also be analysed. In this study, FTIR (Thermo Scientific Nicolet 6700) was done to determine the formation of polyaniline film on the surfaces of the AZ91 magnesium alloy samples.

3.4 Corrosion testing

The potentiodynamic polarisation technique is widely used for the measurement of the corrosion rates of metallic materials and their alloys. The use of this technique also

provides information about the mechanisms involved, such as passivation and localised corrosion in a specific corrosive environment. For corrosion measurement, a potential is applied to measure the corrosion current in the corrosion cell. The potential is applied at an optimal scan rate.

This technique was used to evaluate the performance of the polyaniline coating in a chloride-containing corrosive solution (0.5g/l NaCl). For comparison, bare metal was also tested. In order to understand the effect of the polymerisation agents (potassium hydroxide and sodium salicylate) on the corrosion behaviour of the alloy, potentiodynamic polarisation experiments were also conducted in 0.1 M sodium salicylate ($C_7H_5NaO_3$) and 0.25 M potassium hydroxide (KOH) electrolytes.

The potentiodynamic polarisation experiments were carried out at a 0.5 mV/s scan rate after immersing the sample in the electrolyte for 1 h to establish a relatively stable open circuit potential (OCP). To confirm reproducibility, all the experiments were conducted in triplicate. The degree of protection (DP) of the coatings against corrosion was calculated using Equation (3.1), while the corrosion rate was calculated using Equation (3.2).

$$DP = \frac{i_{corr}(\text{uncoated sample}) - i_{corr}(\text{coated sample})}{i_{corr}(\text{uncoated sample})} \times 100 \quad (3.1)$$

$$CR = \frac{3.27 \times 10^{-3} i_{corr}.\ EW}{D} \quad (3.2)$$

Where:

CR = corrosion rate in mm/year

i_{corr} = corrosion current density (A/cm^2)

EW = equivalent weight

D = density of the metal in g/cm^3.

CHAPTER 4 Electropolymerisation of Aniline on AZ91 Magnesium Alloy: The Effect of Coating Electrolyte Corrosiveness.

This chapter deals with the electropolymerisation of aniline on AZ91 magnesium alloy and the effect of the corrosiveness of the coating electrolyte used. This work has been published in the international journal *Metals* 2017, *7*(12), 533; doi:10.3390/met7120533

4.1 Electrolyte behaviour and corrosiveness

Many surface engineering/coating techniques, such as electroplating, anodisation, micro-arc oxidation, chemical conversion, and polymer coating, have been studied to enhance the corrosion resistance of magnesium and magnesium-based alloys. However, in recent years, conducting polymers have gained much interest for use as corrosion protection coatings on engineering materials, such as steel, copper and magnesium, due to their unique electrical properties. Holness et al. (2005) elaborated the mechanism of polyaniline inhibition of corrosion on iron, explaining why conductive polymers are suitable for the corrosion protection of metals. Further, these conducting polymers can be easily processed and are also economically viable for use as metal coatings. Polyaniline and polypyrrole are the most popular conducting polymers studied as coating materials for the corrosion protection of metals. Iroh and Su (2000) coated polypyrrole on low carbon steel by an electrochemical method. They reported that coatings formed at a relatively low current density exhibited higher corrosion resistance than those formed at a high current density. Similarly, Kazum and Kannan (2013) reported that the electropolymerisation of aniline on steel at 20 mA/cm^2 produced a polyaniline coating that performed better in a chloride-containing solution than one formed at 30 mA/cm^2. They suggested that, at a higher applied current, the inevitable hydrogen evolution hinders coating formation. However, Pawar et al. (2006) reported that a uniform and

strongly adherent polyaniline coating could be formed on mild steel using a cyclic voltammetry coating technique.

Electropolymerisation on a highly reactive metal such as magnesium could be challenging, since the metal may dissolve during the coating process if the electrolyte is corrosive. The literature suggests that salicylate solution is widely used as a polymerisation agent for polyaniline and polypyrrole formation on steel and copper (Cascalheira et al., 2003, 2008; Pawar et al., 2006; Sitaram et al., 1997). Since salicylate solution is slightly acidic in nature, which can be corrosive to magnesium, some researchers have attempted to polymerise pyrrole (Jiang et al., 2003) and aniline (Guo et al., 2003) on magnesium alloys in an alkaline medium. Although the two studies achieved successful polymerisation on magnesium alloys in an alkaline medium, the corrosion protection properties were either not investigated or were inconclusive. It is well known that magnesium passivates in alkaline medium (Song et al., 2003, 2005), but to the authors' best knowledge, the effect of such passivation on polymerisation has not been studied. Hence, it is worthwhile to study the effect of the corrosiveness of coating electrolytes on the polymerisation and corrosion resistance of polymer coatings on magnesium-based materials.

In this study, two electrolytes of different corrosiveness were used to electropolymerise aniline on a magnesium alloy. The coating performance was evaluated using the potentiodynamic polarisation technique in a chloride-containing solution.

4.1.1. Effect of pH on metal substrate

A potentiodynamic polarisation plot of a bare sample tested in potassium hydroxide and sodium salicylate is shown in Figure 4.1.

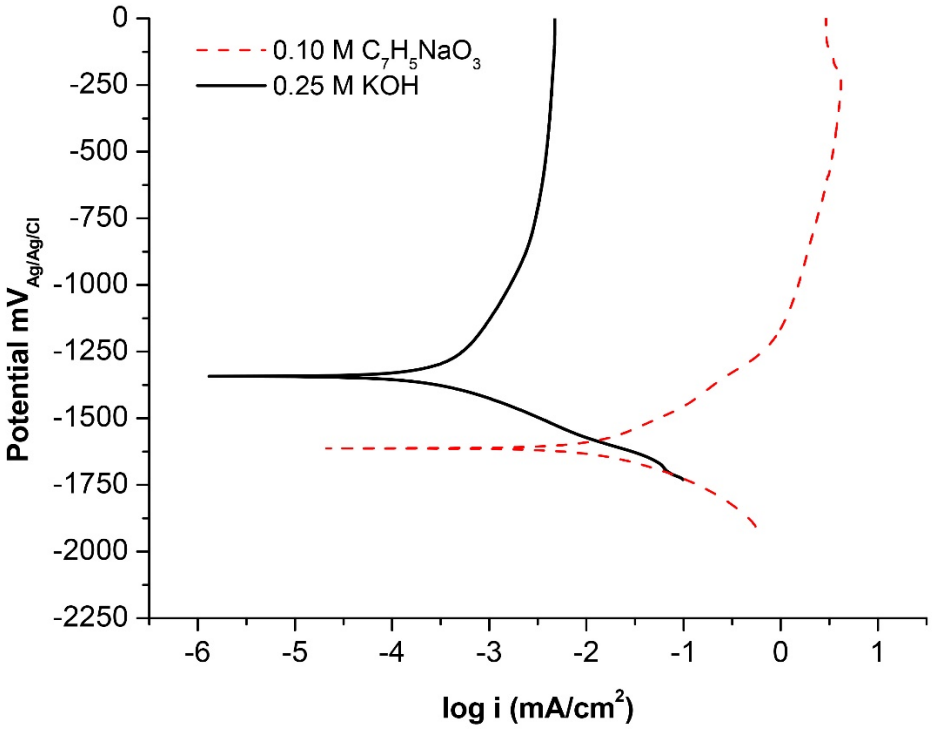

Figure. 4.1 Potentiodynamic polarisation curves of AZ91 magnesium alloy in 0.25 M potassium hydroxide and 0.1 M sodium salicylate electrolytes

The corresponding electrochemical data used in Figure 4.1 is presented in Table 4.1. The E_{corr} of the alloy in potassium hydroxide was ~275 mV noble as compared to sodium salicylate. The cathodic and anodic polarisation curves for the alloy in potassium hydroxide occurred at lower currents than those for sodium salicylate. Passivity in the anodic curve was evident in the potassium hydroxide case, whereas in salicylic acid, the dissolution of the alloy was significant. As a result, the corrosion current (i_{corr}) in sodium salicylate was close to two orders of magnitude higher than that in potassium hydroxide. The calculated corrosion rates for the alloy in sodium salicylate and potassium hydroxide were 0.887 and 0.011 mm yr^{-1}, respectively. The lower corrosion rate in potassium hydroxide, which is an alkaline medium (pH = 12.03), can be attributed to the formation of a protective film on the alloy's surface. However, in the acidic sodium salicylate

solution (pH = 5.81), corrosion of the alloy was severe. Post-corrosion optical microscopy images are shown in Figure 4.2.

Table 4.1 Electrochemical corrosion data for AZ91 magnesium alloy in two different electrolytes

Parameter	0.10 M Sodium salicylate	0.25 M Potassium hydroxide
E_{corr} (mV)	-1611 ± 4.95	-1335 ± 11
i_{corr} (μA/cm^2)	19.23 ± 1.61	0.2509 ± 0.014
Corrosion rate (mm yr^{-1})	0.887	0.011
pH	5.81 ± 0.16	12.03 ± 0.02

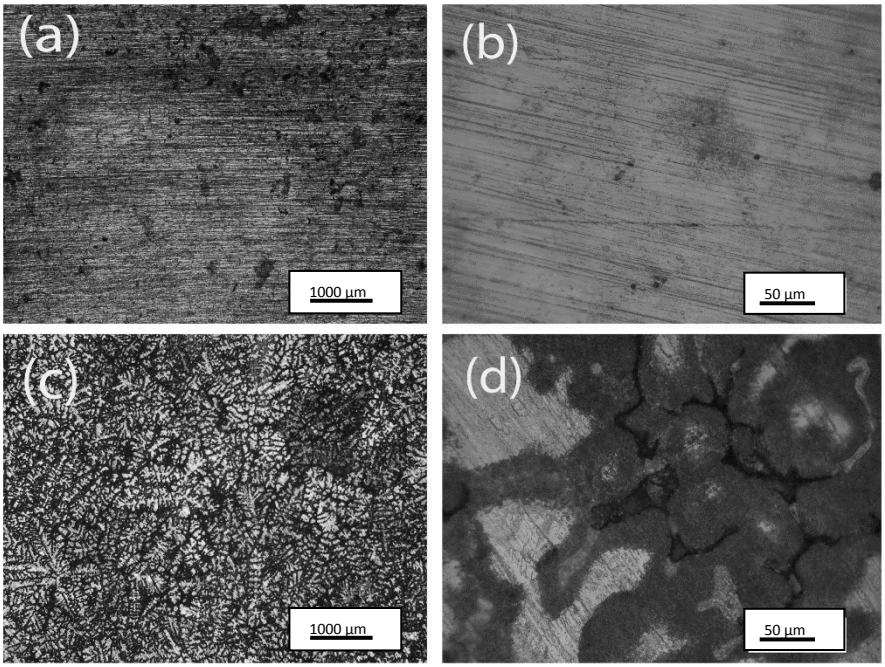

Figure 4.2 Optical micrographs of AZ91 magnesium alloy after potentiodynamic polarisation experiments in: (a, b) 0.25 M potassium hydroxide, and (c, d) 0.1 M sodium salicylate

4.1.2. Post-corrosion optical microscopic analysis without polyaniline coating

During the potentiodynamic polarisation tests, the AZ91 magnesium alloy samples showed different corrosive behaviours in the oxidising electrolytes, which can be seen in

Figure 4.2. The alloy tested in potassium hydroxide electrolyte exhibited a passive layer which, in fact, protected the alloy from corrosion. The passive layer was $Mg(OH)_2$, the formation of which can be described by the following equation:

$$Mg + 2H_2O \rightarrow Mg(OH)_2 + H_2 \qquad (4.1)$$

Very few signs of corrosion can be seen on the alloy surface, whereas in sodium salicylate, the alloy exhibited high corrosion attack, and secondary phase particles in the alloy were clearly revealed. It appears that the corrosion started near the secondary phase particle regions, where the aluminium content was lean, and then propagated outwards.

4.2 Polymer Coating

Polyaniline was coated on AZ91 magnesium alloy using an electropolymerisation technique, and the corrosive effects of the coating electrolytes on polymerisation and coating performance were evaluated. Two electrolytes, aniline + sodium salicylate (PASS) and aniline + potassium hydroxide (PAPH), of different corrosiveness were used for polyaniline coating on AZ91 magnesium alloy. The degradation behaviour of the coated alloy was analysed using potentiodynamic polarisation tests.

Cyclic voltammetric curves for the alloy in the PASS and PAPH electrolytes are shown in Figure 4.3 and insight is PAPH cyclic voltammetric response. In PASS electrolyte, which contained an acidic sodium salicylate, the first-forward cycle showed strong magnesium oxidation until ~0.75 V, above which oxidation of aniline started to occur. However, in subsequent forward cycles, magnesium oxidation was insignificant due to the formation of polyaniline, which occurred during the reverse cycles.

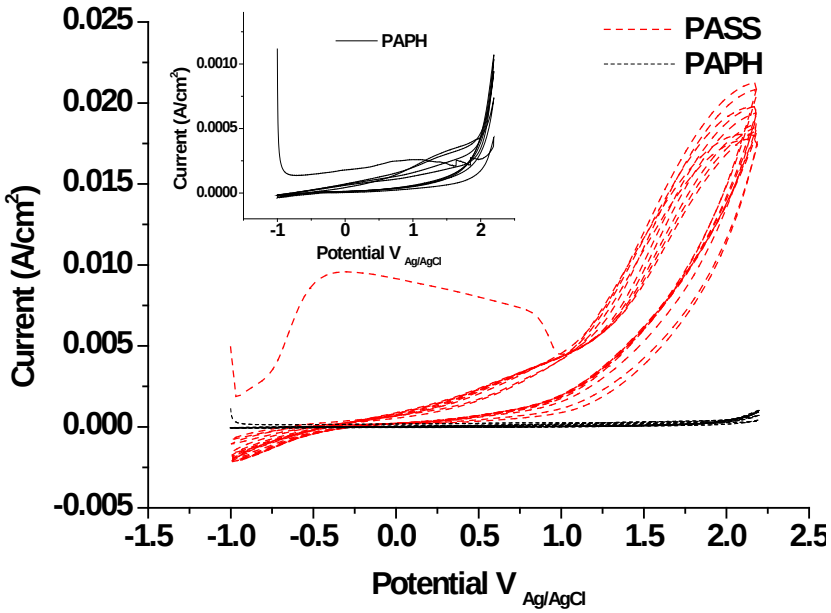

Figure 4.3 Cyclic voltammetry response of AZ91 magnesium alloy in PASS (aniline + sodium salicylate) and PAPH (aniline + potassium hydroxide) electrolytes. Insight is PAPH cyclic voltametric response.

The peak anodic current density at 2 V decreased with increasing numbers of cycles, confirming the growth of the polyaniline coating. In the PAPH electrolyte, which contained strongly alkaline potassium hydroxide, there was little dissolution of magnesium during the first-forward cycle. Based on the anodic peak current density, it can be said that the oxidation of aniline was significantly lower in the PAPH electrolyte that in the PASS electrolyte. Further, it was noted that the peak current increased as the number of cycles increased in the PAPH electrolyte, which is in contrast to that observed in the PASS electrolyte. The anodic protective layer formed in the PAPH electrolyte minimized the oxidation of aniline and, hence, the formation of polyaniline was not significant.

With the two different oxidizing agents (i.e. aniline + sodium salicylate, PASS; and aniline + potassium hydroxide, PAPH), the polymer coatings exhibited different

morphologies, thicknesses and adhesion characteristics. Table 4.2 shows the coating thickness and adhesion strength results for the AZ91 magnesium alloy. A thicker coating was produced in the PASS electrolyte (~ 9 µm) than in the PAPH electrolyte (~ 3 µm). Visual observation of the PASS-coated alloy found a dark greenish colour, while the PAPH-coated alloy exhibited a light yellowish colour. Coating adhesion strength was ~ 2 N/mm^2 for PASS, whereas for PAPH it was too low to measure.

Table 4.2. Thickness and adhesion strength of the coatings formed on AZ91 magnesium alloy in two different electrolytes

Parameter	PASS coating	PAPH coating
Thickness (µm)	8.75 ± 0.24	2.75 ± 0.04
Adhesion (N/mm^2)	1.95 ± 0.07	Immeasurable

4.2.1 Optical microscopy analysis of polyaniline-coated samples

The optical micrographs of the coatings are shown in Figure 4.4 (a-d). The PAPH coating was thin, such that polishing scratches can be seen on the alloy (Fig. 4.5 b). The PASS coating, however, exhibited a scattered pore-like morphology and did not display any polishing scratches (Fig. 4.5 c). A similar pore-like morphology has been reported for polyaniline coatings on steel, which has been attributed to an oxygen evolution reaction at high anodic potentials. However, in magnesium, the observation could also be due to a hydrogen evolution reaction, even at a relatively low anodic potential.

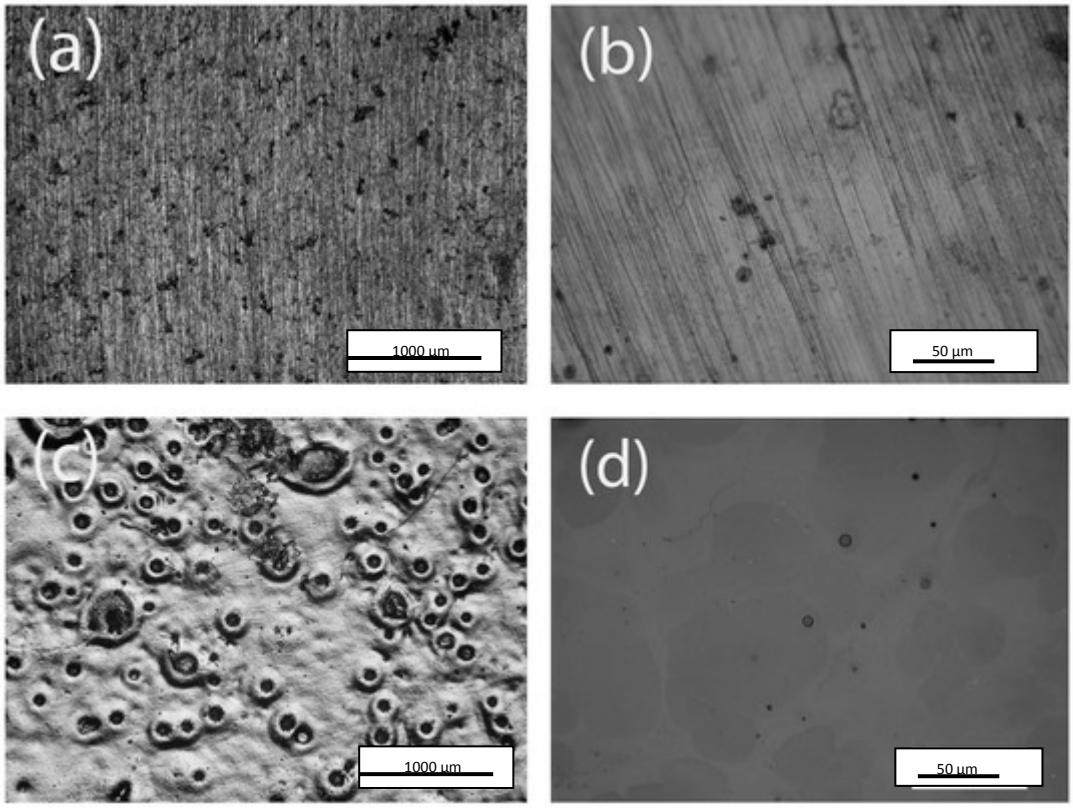

Figure 4.4 Optical micrographs of the coated AZ91 magnesium alloy: (a, b) PAPH coated, and (c, d) PASS coated

4.2.2 Coating thickness and FTIR analysis

Coating thickness was measured by a thickness gauge (Fisher Dualscope MP0R), and chemical formation was analysed by Fourier transform infrared spectroscopy (FTIR; Figure 4.5). The FTIR spectra confirmed the presence of polyaniline, with PASS samples showing strong bands at 1000–1800 cm^{-1} [15], which were slightly weaker in PAPH samples. Based on colour and thickness measurements, it can be suggested that the PAPH coating was largely magnesium hydroxide with a thin polyaniline top layer.

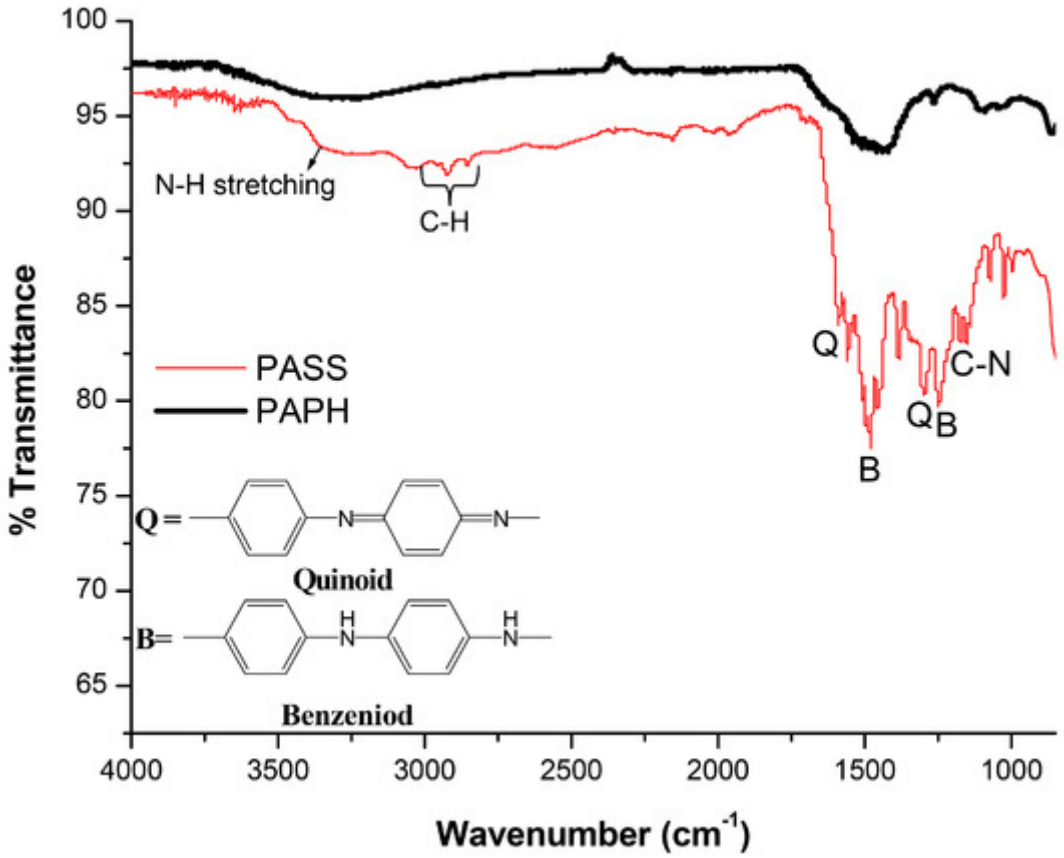

Figure 4.5 FTIR analysis of PASS and PAPH coatings.

4.3 Potentiodynamic Polarisation

The corrosion resistance of the coatings of the two types of AZ91 magnesium alloy samples (coated in polyaniline with different electrolytes) was tested in a chloride-containing solution. Figure 4.7 shows the potentiodynamic polarisation curves of the PASS- and PAPH-coated alloys in comparison with bare alloy in a chloride-containing solution. The corresponding electrochemical data are presented in Table 4.3. The corrosion potential (E_{corr}) of the coated alloy samples shifted towards the active direction relative to that of bare alloy. The bare alloy did not show any breakdown potential (E_{bd}) in the anodic curve, while the coated alloy samples did. The i_{corr} of the PASS-coated alloy was almost an order of magnitude lower than that of bare alloy. Interestingly, the PAPH-coated alloy showed a higher i_{corr} value compared to the bare alloy, but showed

some passivity effect in the anodic polarisation curve. The corrosion rates of the bare alloy, and PASS- and PAPH-coated alloy samples, were 0.051, 0.0086 and 0.125 mm yr^{-1}, respectively. The degree of protection (DP) provided by the PASS coating was ~83%.

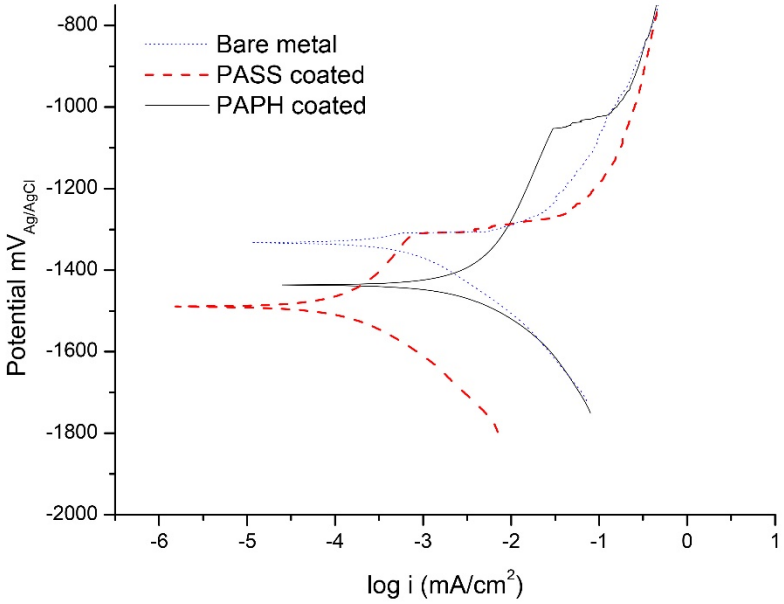

Figure 4.6 Potentiodynamic polarisation curves of bare and coated AZ91 magnesium alloy samples in chloride-containing solution

Table 4.3. Electrochemical corrosion data of bare and coated AZ91 magnesium alloy in chloride-containing solution

Parameter	Bare metal	PASS-coated	PAPH-coated
E_{corr} (mV)	-1296 ± 63.23	-1473 ± 20.04	-1428 ± 12.73
E_{bd} (mV)	Not observed	-1299 ± 14.14	1145 ± 131.52
i_{corr} (μA/cm^2)	1.03 ± 0.28	0.19 ± 0.01	2.71 ± 0.33
Corrosion rate (mm yr^{-1})	0.051	0.0086	0.125
Degree of protection	Not observed	83.17 %	Not observed

4.3.1 Post-corrosion analysis

Post-corrosion micrographs of the bare and coated alloy samples are shown in Fig. 4.7. The coatings minimised localised corrosion attack of the alloy. The bare alloy exhibited

extensive localised corrosion throughout the sample (Fig. 4.7 a), whereas the PAPH-coated alloy revealed pockets of localised corrosion (Fig. 4.7 c). However, the PASS-coating sample showed no recognisable corrosion attack. It should be noted that the uneven morphology of the PASS-coated alloy (Fig. 4.7 c) is simply the coating morphology, as seen in Fig. 4.7 c.

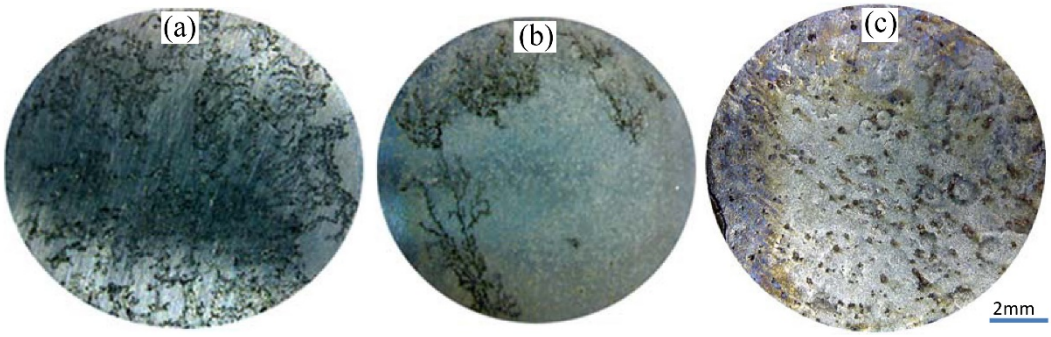

Figure 4.7 Post-corrosion micrographs of AZ91 magnesium alloy: (a) bare, (b) PASS-coated, and (c) PAPH-coated, after potentiodynamic polarisation in chloride-containing solution

Table 4.4 shows the pH of the coating electrolytes used, and the pH of the corrosion test solutions before and after the potentiodynamic polarisation experiments. The PASS and PAPH coating electrolytes exhibited pH values of 6.52 and 12.08, respectively. Note that the corrosion test solution turned alkaline after the potentiodynamic polarisation experiments with the bare and PAPH-coated alloys; in both cases, the pH changed from ~6.6 to ~8.8. This increase in pH indicates that there was magnesium dissolution. However, the pH of the electrolyte used with the PASS-coated alloy did not change significantly after the corrosion test.

Table 4.4 pH of coating electrolytes, and corrosion test solutions before and after corrosion testing

Sample	Coating electrolyte pH	Corrosion test solution pH	
		Before test	After test
Bare alloy	N/A	6.56 ± 0.26	8.78 ± 0.08
PASS-coated alloy	6.52 ± 0.20	6.67 ± 0.08	6.73 ± 0.05
PAPH-coated alloy	12.08 ± 0.02	6.65 ± 0.06	8.76 ± 0.02

4.4 Reaction mechanism of aniline

The reaction mechanism of aniline electropolymerisation is presented in Figure 4.8. The first-step (I) of the polymerisation process of aniline involves formation of aniline cation radicals by anodic oxidation on the electrode surface in an acidic solution. In the PASS electrolyte (Figure 4.4), significant dissolution of the alloy can be observed at potentials starting from −0.75 V, which can be attributed to the relatively low pH (6.52) of the coating electrolyte. In fact, the low pH of the electrolyte catalyses the formation of aniline cation radicals. Cascalheira et al. 2003, reported that in the electropolymerisation of pyrrole on copper metal, salicylate ions form a copper salicylate complex on the metal surface which facilitates polypyrrole formation. A similar mechanism is plausible for polyaniline formation on AZ91 magnesium alloy, i.e., a magnesium salicylate complex promotes aniline polymerisation. The subsequent polymerisation reactions involve coupling of the anilinium radicals and formation of a dimer (II), further oxidation (III) and chain propagation by coupling reactions (IV). As can be seen in Figure 4.4 for the PASS coating, the increase in the current density starting at 1.0 V in the first sweep is due to the oxidation of aniline, and after reaching 2 V, the reverse potential produces polyaniline. The decrease in the anodic peak current density from cycles 1 to 5 can be attributed to the growth of the polymer coating, which was evident from the optical

micrographs (Figure 4.5) and FTIR spectra (Figure 4.6). In the case of the PAPH electrolyte (Figure 4.4), a strongly alkaline medium (pH 12.08), the anodic current density in the first sweep was lower than in the PASS electrolyte, which suggests that the rate of magnesium dissolution decreased due to the immediate formation of a passive layer. The peak current increased as the number of cycles increased, suggesting slow formation of polyaniline. Thus, the results suggest that a passive layer formed on the AZ91 magnesium alloy in the alkaline PAPH electrolyte reduced the rate of aniline cation radical formation and, consequently, decreased the polymerisation process. The relatively corrosive PASS electrolyte, however, formed a thicker polyaniline coating on the AZ91 samples that provided significant corrosion protection.

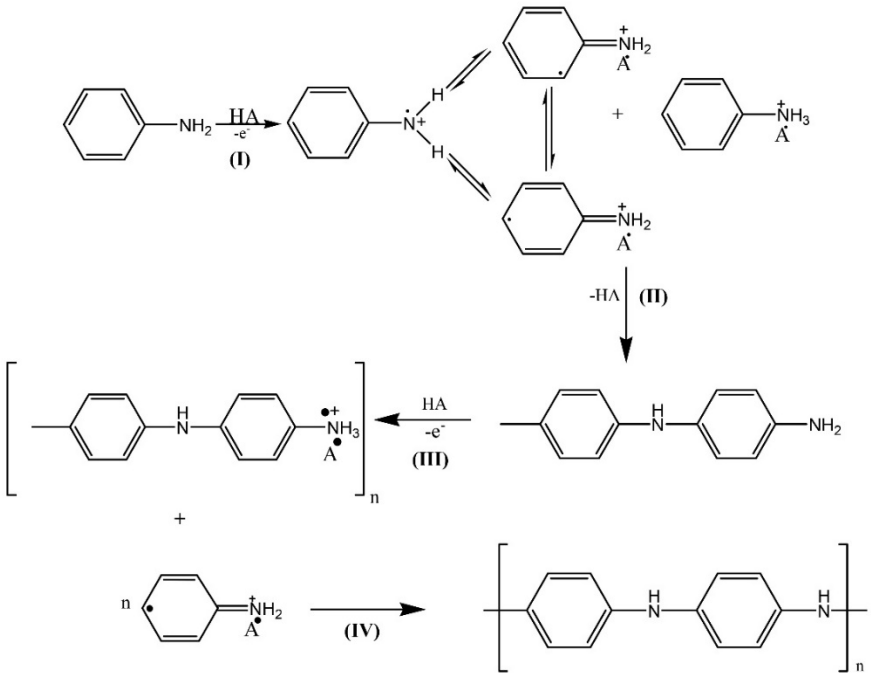

Figure 4.8 Electropolymerisation mechanism of aniline to polyaniline.

4.5 Summary

- Polyaniline coating in an aniline + sodium salicylate (PASS) electrolyte produced a better coating than that produced in an aniline + potassium hydroxide (PAPH) electrolyte.
- The corrosion resistance provided by the PASS coating was significant compared to that of bare alloy.
- Post-corrosion analysis revealed minimal corrosion attack in the PASS-coated alloy in comparison with the PAPH-coated alloy.
- The results suggest that the relatively high corrosiveness of the PASS-coating electrolyte did not adversely affect the formation and performance of the polyaniline coating on the AZ91 magnesium alloy.
- The passive film formed on the AZ91 magnesium alloy in the alkaline PAPH electrolyte lessened the polymerisation process.

CHAPTER 5 Galvanostatic Polymerisation of Aniline on AZ91 Magnesium Alloy: Evaluating the Corrosion Protection Behaviour in Chloride-containing Solution

In this study, polyaniline was coated on AZ91 magnesium alloy using a galvanostatic method. The galvanostatic coating was performed at various constant current densities to understand the effect of current density on coating formation. The morphology, thickness, adhesion and corrosion resistance of coatings subjected to a chloride-containing environment were examined.

5.1 Galvanostatic coating

An aniline and sodium salicylate electrolyte bath was used to coat polyaniline onto AZ91 magnesium alloy at ambient temperature and various current densities.

5.1.1 Effects of current density at 14, 18 and 20 mA/cm^2

Current density affects electrodeposited coating formation; however, forming coatings on metallic materials with an active or anodic electromotive force (emf) is a challenge. The galvanostatic curves for the alloy in the polyaniline and sodium salicylate electrolyte are shown in Figure 5.1. This transient potential vs. elapsed time plot for the electropolymerisation of aniline using the galvanostatic technique at constant currents of 14, 18 and 20 mA/cm^2 describes the dissolution of the metal and oxidation of the polymer. Electrodeposition of the polymer was carried out for 600 seconds for each sample. The plot for the sample coated at 14 mA/cm^2 showed a sharp increase in potential (−0.072 to 3.45 V) with time. The galvanostatic curve shows magnesium oxidation at ~3.45 to ~4.45 V, then the potential remained stable between ~3.45 to ~4.45 V for the remainder of the experiment. After the first 30 seconds, the metal substrate gradually changed colour from silvery to black due to coating formation. Gas bubbles appeared on

the surface of the metal at a slow rate within ~10–15 seconds of test commencement, and continued throughout the coating period.

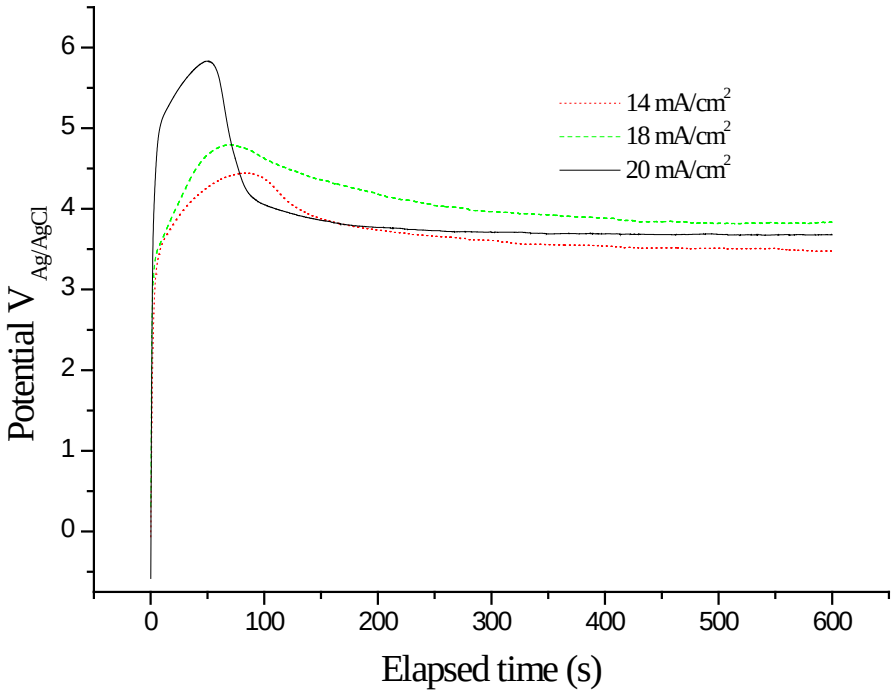

Figure 5.1. Galvanostatic response of AZ91 magnesium alloy in 0.3 M aniline and 0.1 M sodium salicylate solution.

During coating at 18 mA/cm^2, a wide curve started at ~3.6 V in the first ~100 seconds. Compared to the 14 and 20 mA/cm^2 processes, the gradual decrease of potential at 18 mA/cm^2 was very slow and continued to drop to ~3.8 V for the remainder of the test. Gas bubble production was substantially higher and the colour of the substrate's surface changed rapidly. The plot for the 20 mA/cm^2 coating test shows that the potential increased from ~0.6 V and continued to rise to ~5.84 V with time. Gas bubble production was significantly higher again, with small but frequent bubbles. The colour of the substrate also changed faster than at 18 and 14 mA/cm^2. Further, it was noted that the

peak potentials increased with increasing current density. The potentials in all three coating tests remained relativity stable at ~3.47–3.84 V.

5.1.2 Coating morphology at different current densities

Figure 5.2 shows SEM images of the polyaniline coatings obtained at 14, 18 and 20 mA/cm^2 current densities. Coatings formed at 14 mA/cm^2 exhibited large pores; however, samples coated at 18 mA/cm^2 had relatively smooth surfaces. The coating performed at 20 mA/cm^2 also had a smooth surface. Hence, the polyaniline coating improved morphologically with increasing current density.

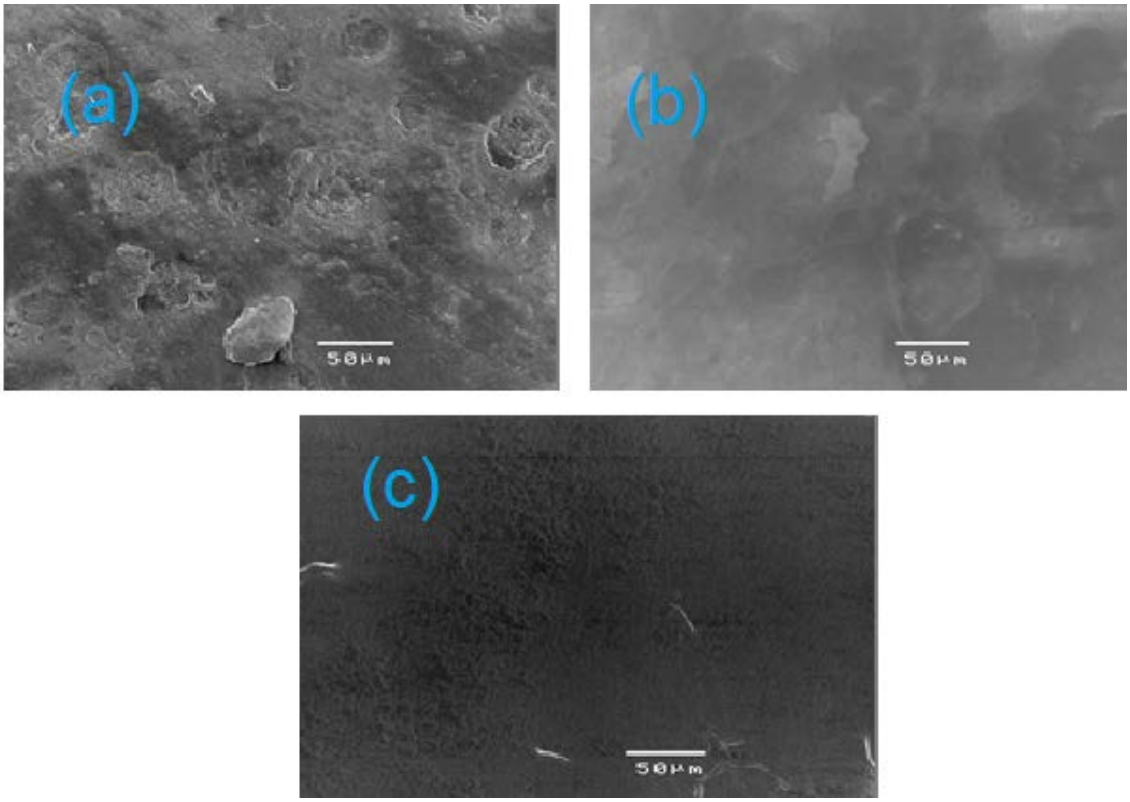

Figure 5.2. SEM images of samples coated at current densities of (a) 14 mA/cm^2; (b) 18 mA/cm^2; and (c) 20 mA/cm^2 before potentiodynamic polarisation testing.

5.1.3 FTIR analysis at different current densities

The FTIR spectra of the samples coated at 14, 18 and 20 mA/cm^2 are shown in Figure 5.3. They are all similar, revealing that the chemical composition of the coatings was the same. The spectral peak at 1598 cm^{-1} indicates that there was quinoid (Q) ring stretching in all three samples (Guo et al., 2003; Kazum and Bobby 2013). The bands at 1494 cm^{-1} and 1385 cm^{-1} correspond to stretching of benzoid (B) rings (Kazum and Bobby 2013). The oxidising agent sodium salicylate belongs to carboxylic group, the presence of salicylate acid in the coating was observed at the 1265 cm^{-1} band (Pawar et al., 2006).The spectral peaks of the Q and B bands indicate that polyaniline coatings were formed on all three samples at different current densities. Further, the bands at 1177 cm^{-1} and 1023 cm^{-1} indicate 1–4 substitution on benzene rings, while the bands between 800 cm^{-1} and 700 cm^{-1} were indicative of 1–3 substitutions (Pawar et al., 2006).

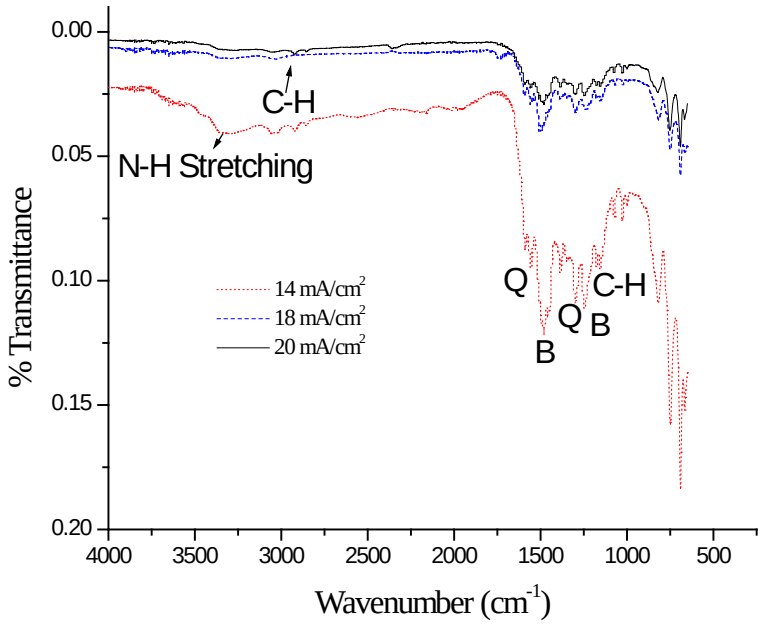

Figure 5.3. FTIR analysis of polyaniline coating on AZ91 magnesium alloy at 14, 18 and 20 mA/cm^2 current densities

Table 5.1. Thickness and adhesion of polyaniline coatings formed at 14, 18 and 20 mA/cm^2 current densities in 0.3 M aniline and 0.1 sodium salicylate

Coating parameter	**14 mA/cm^2**	**18 mA/cm^2**	**20 mA/cm^2**
Thickness (µm)	11.99 ± 2.84	12.89 ± 1.117	17.54 ± 3.33
Adhesion test (N/mm^2)	0.65 ± 0.070	0.7 ± 0.14	0.95 ± 0.071

Table 5.1 shows measurements of coating thickness and adhesion. Coating thickness increased with current density: the thicknesses obtained at 14, 18 and 20 mA/cm^2 were 11.99 ± 2.84 µm, 12.89 ± 1.117 µm and 17.54 ± 3.33 µm, respectively. Higher current density increased the redox rate at the metal-electrolyte interface, which enhanced polymerisation (Kazum and Bobby 2013). However, at high current density, bubble formation also increased. Interestingly, adhesion also increased with current density.

5.2 Potentiodynamic polarisation

The AZ91 magnesium alloy samples, both bare and coated in polyaniline at three current densities, were tested for corrosion resistance in chloride-containing solution. Figure 5.4 shows their potentiodynamic polymerisation curves. The results reveal that the anodic curve of bare alloy showed breakdown potential; however, the sample coated at 18mA/cm^2 had very minor breakdown potential and at sample coated at 14 mA/cm^2 had none. The breakdown potential most likely occurred due to pitting corrosion and breakdown of coating film.

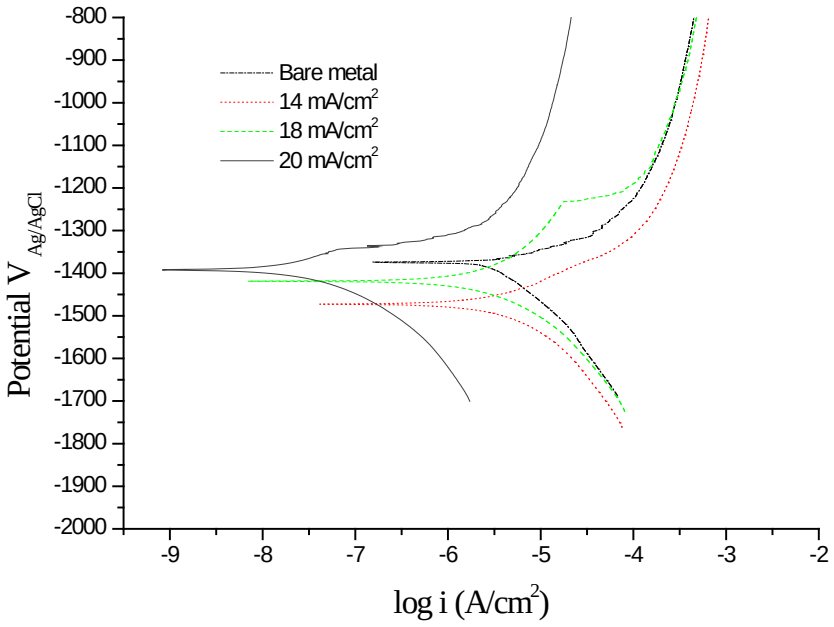

Figure 5.4. Potentiodynamic polarisation curves of bare and coated AZ91 magnesium alloy samples in chloride-containing solution

Table 5.2. Electrochemical corrosion data of bare and coated AZ91 magnesium alloy in chloride-containing solution

Parameter	**Bare**	**Coated at 14 mA/cm^2**	**Coated at 18 mA/cm^2**	**Coated at 20 mA/cm^2**
E_{corr} (mV)	−1424 ± 8.5	−1459 ±70	−1401 ± 1.41	−1447.5 ± 74.25
i_{corr} (µA/cm^2)	3.45 ± 0.44	3.28 ± 1.36	1.8 ± 0.028	0.081 ± 0.029
Corrosion rate (mm yr^{-1})	0.159	0.151	0.083	0.0028

Table 5.2 shows potentiodynamic polymerisation test results, which reveal that the corrosion resistance of the coatings increased with current density. The gradual decrease in i_{corr} with current density reveals that with increasing current density, the coatings become increasingly uniform and resistant to the chloride-containing solution. The corrosion rates reveal that the coating obtained at 20 mA/cm^2 had the lowest corrosion

rate (0.0028 mm yr^{-1}), while the coating obtained at current density 14 mA/cm^2 had a high rate (0.151 mm yr^{-1}) that was similar to that of bare alloy.

Figure 5.5 shows the degree of protection provided by coatings produced at 14, 18 and 20 mA/cm^2. The highest corrosion protection was ~97%, which was obtained at 20mA/cm^2, followed by ~48% and ~ 5% achieved at 18 and 14 mA/cm^2, respectively.

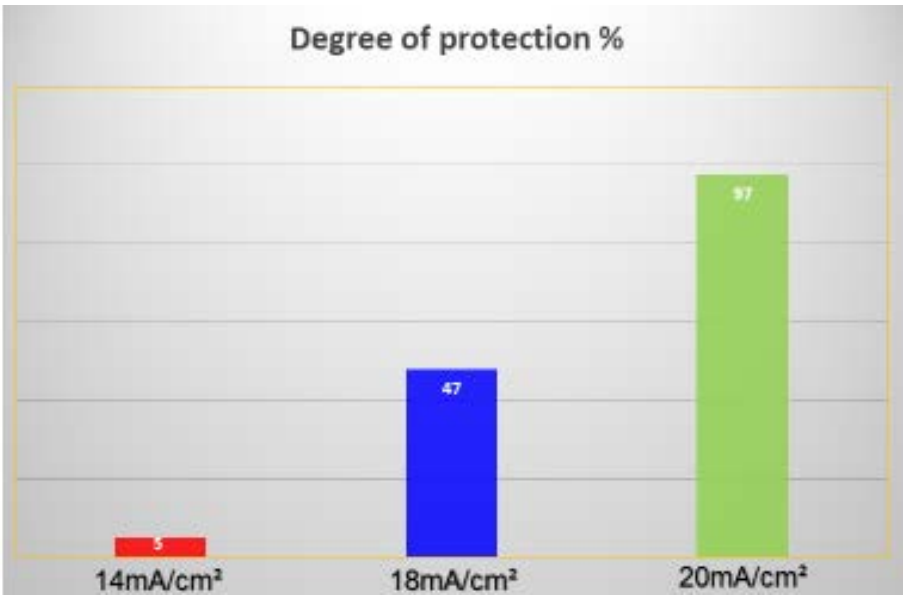

Figure 5.5. Degree of protection of samples coated at 14, 18 and 20 mA/cm^2

5.3 Summary

- Polyaniline coatings were produced on AZ91 alloy by a galvanostatic technique at current densities of 14, 18 and 20 mA/cm^2.
- Coating performance was investigated using potentiodynamic polarisation tests in a chloride-containing environment.
- The polyaniline coatings protected the alloy from corrosion. This protective effect increased according to the current density at which the coating was produced.
- At low current density, the coating obtained was not uniform and provided little corrosion protection; conversely, at high current density, the coating was uniform, had fewer defects and provided good protection.

CHAPTER 6 Electropolymerisation of Aniline on Alkaline Pre-treated Magnesium Alloy and Corrosion Evaluation

This chapter describes the electropolymerisation of aniline on alkaline pre-treated magnesium alloy and evaluates the corrosion behaviour of the coated alloy. This work was published in the *Australasian Corrosion Association Conference Proceedings, 2017*.

6.1 Magnesium passivation

Magnesium is a reactive metal and forms a magnesium oxide/hydroxide protective layer in natural environments. However, due to the Pilling-Bedworth ratio being < 1, the oxide/hydroxide protective layer on the surface of the metal is thin and unstable; hence, it cannot protect the metal from corrosion in corrosive environments (Samaniego et al., 2014). Some magnesium alloys may form oxide/hydroxide films with Pilling-Bedworth ratios > 1. Figure 6.1 refers the pH values for magnesium oxide/hydroxide protective layer is alkaline environment and dissolution of the layer < 11 pH. (Feliu et al., 2011; Taheri et al., 2012)

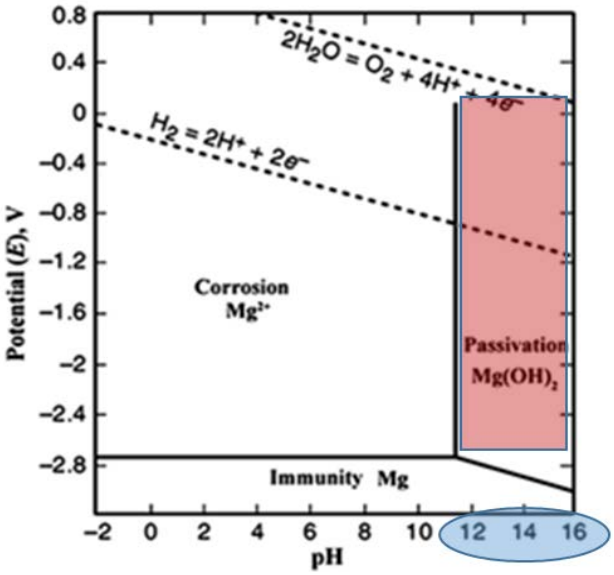

Figure 6.1. Poubaix diagram of magnesium showing its corrosion and passivation at different pHs

6.1.1 Potentiostatic passivation

Pre-treatment of AZ91 magnesium alloy samples was conducted in a 3 M sodium hydroxide solution to enhance coating formation and passivation by applying a constant potential. Pre-treatment was conducted at −750 mV and −195 mV.

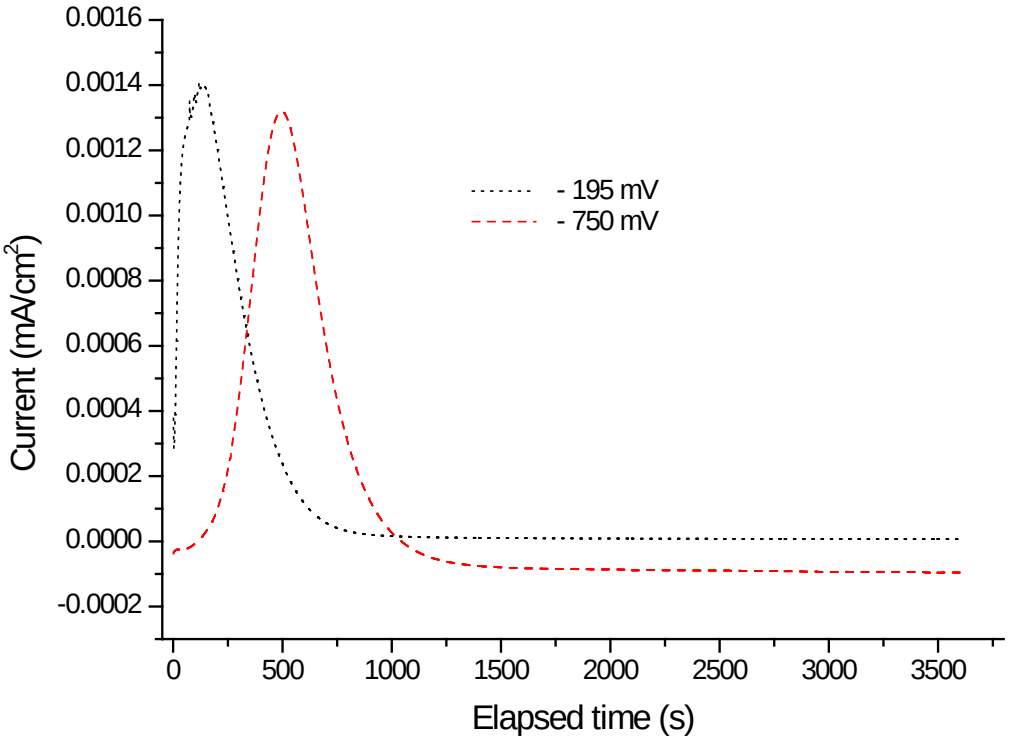

Figure 6.2 Transient potential current vs. time curves for pre-treatment of 3 M sodium hydroxide on AZ91 magnesium samples.

Figure 6.2 shows the transient graph of current vs. elapsed time of the samples treated in 3 M NaOH. The curves reveal that the samples pre-treated at −195 mV and −750 mV had sharp increases in current of ~1.4 mA and ~1.3 mA, respectively. The peaks for both pre-treated samples had different timings: ~85 seconds at −195 mV and ~600 seconds at −750mV. The current sharply decreased at 0 mA throughout the 60 minute pre-treatment period for both pre-treated samples.

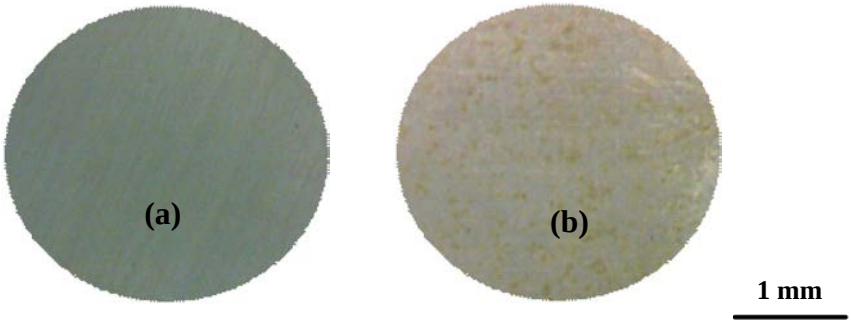

Figure 6.3 Macrographs of (a) bare sample and (b) −195 mV pre-treated sample in 3 M sodium hydroxide solution

Figure 6.3 shows macrographs of bare AZ91 magnesium alloy samples and those pre-treated in 3 M NaOH solution at −195 mV for one hour. The image reveals that the sample pre-treated at −195 mV exhibited a whitish surface, confirming the formation of a magnesium hydroxide layer.

6.2 Cyclic Voltammetry Coating on Pre-treated AZ91 Magnesium Alloy Samples

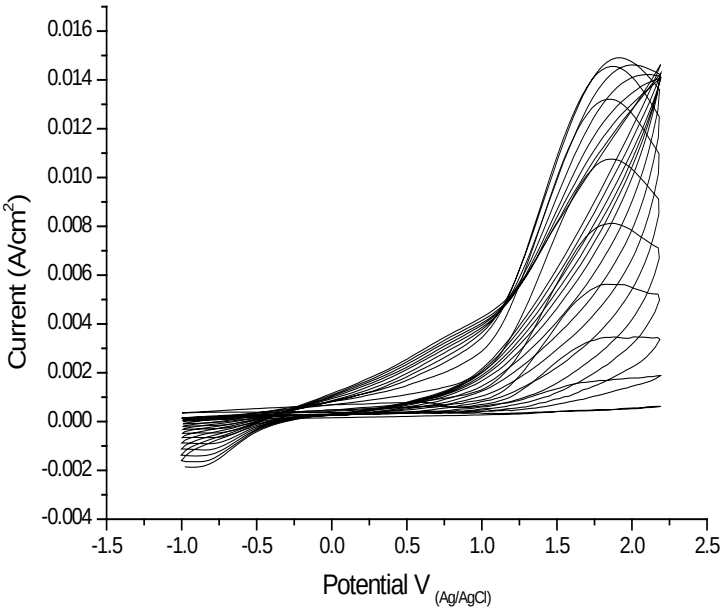

Figure 6.4 Cyclic voltammetry curves of alkaline pre-treated AZ91 magnesium alloy in 0.3 M aniline and 0.1 M sodium salicylate solution

The cyclic voltammetry curve for 3 M NaOH alkaline pre-treated AZ91 magnesium alloy coated in 0.3 M aniline and 0.1 M sodium salicylate solution is shown in Figure 6.4. The curves reveal that the first cycle of the alloy exhibited a low peak current density of ~0.002 A/cm^2, which can be attributed to passive film formation on the alloy. However, the current density gradually increased with each cycle as the polymer coating formed. In a previous chapter (Chapter 4), during cyclic voltammetry with the 0.3 M aniline and 0.1 M sodium salicylate solution, the first-forward cycle showed a significant increase in current density of ~0.010 A/cm^2. The broad anodic current curve showed strong magnesium oxidation until ~0.75 V, above which oxidation of aniline started to occur.

Based on the anodic peak current densities of pre-treated and non-pretreated samples coated in 0.3 M aniline and 0.1 M sodium salicylate solution, it can be said that the oxidation of aniline in the alkaline pre-treated sample was significantly lower that in the non-pre-treated sample. Further, it was noted that the peak current increased with increasing numbers of cycles in the pre-treated samples, which is in contrast to that observed in the non-pretreated samples.

6.3 Corrosion analysis

Corrosion analysis was carried out to determine the effects of pre-treatment with 3 M sodium hydroxide on aniline coatings of AZ91magnesium alloy. This analysis observed the morphology, corrosion resistance and degree of protection provided by polyaniline coatings following pre-treatment with 3 M NaOH solution.

6.3.1 Potentiodynamic polarisation test

Potentiodynamic polarisation tests were performed to gain further insight into the effects of alkaline pre-treatment and polyaniline coating on the corrosion behaviour of AZ91

magnesium alloy. Plots of the curves of the bare and polyaniline-coated AZ91 magnesium alloy samples in 0.5 g/L NaCl solution are shown in Figure 6.5. The corresponding data of the potentiodynamic polarisation tests are shown in Table 6.1. The corrosion current density (i_{corr}) of the coated alloy was 0.177 µA/cm^2, while for bare metal it was 1.03 µA/cm^2. The sample pre-treated in 3 M NaOH and coated in 0.3 M aniline and 0.1 M sodium salicylate solution reduced the corrosion current by an order of magnitude. The degree of protection provided by the polymer was ~83%.

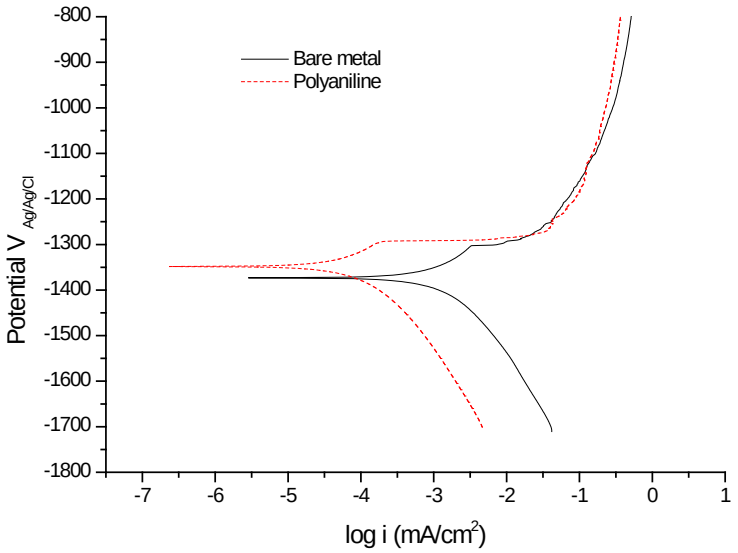

Figure 6.5 Potentiodynamic polarisation curves of Bare AZ91 magnesium alloy sample and pre-treated in 3 M NaOH, coated in polyaniline and tested in 0.5 g/l sodium chloride solution

Table 6.1. Electrochemical corrosion data from the potentiodynamic polarisation curves of bare and pre-treated, polyaniline-coated alloy in 0.5 g/L NaCl solution

Parameter	Bare alloy	Polyaniline-coated alloy
E_{corr} (mV)	−1296 ± 63.23	−1349.4 ± 79.37
i_{corr} (µA/cm^2)	1.03 ± 0.28	0.177 ± 0.08
Corrosion rate (mm yr^{-1})	0.051	0.0081
Degree of protection (%)	N/A	82.81

6.3.2 Macroscopic analysis

Figure 6.6 shows macrographs of the coated alloy before and after potentiodynamic polarisation in 0.5 g/L NaCl solution. The macrograph of the sample before polarisation reveals no visible pores in the coating. However, after potentiodynamic polarisation, the coating showed evidence of delamination. White corrosion products were also visible. This suggests that alkaline pre-treatment is not a suitable step for electropolymerisation of aniline on magnesium alloy. The bonding between the hydroxide/oxide layer and polymer was weak and hence failed after polarisation.

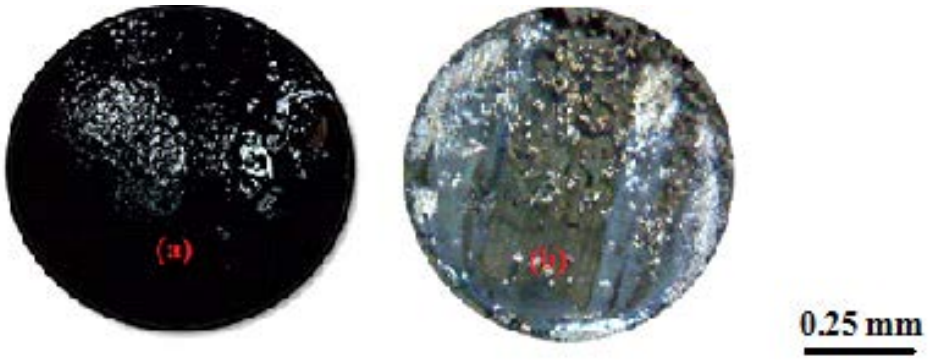

Figure 6.6 Micrographs of sample (a) before (b) after potentiodynamic polarisation of samples pre-treated in 3 M NaOH solution and coated in 0.1 aniline and 0.3 M sodium salicylate electrolyte

6.3.3 Coating delamination mechanism

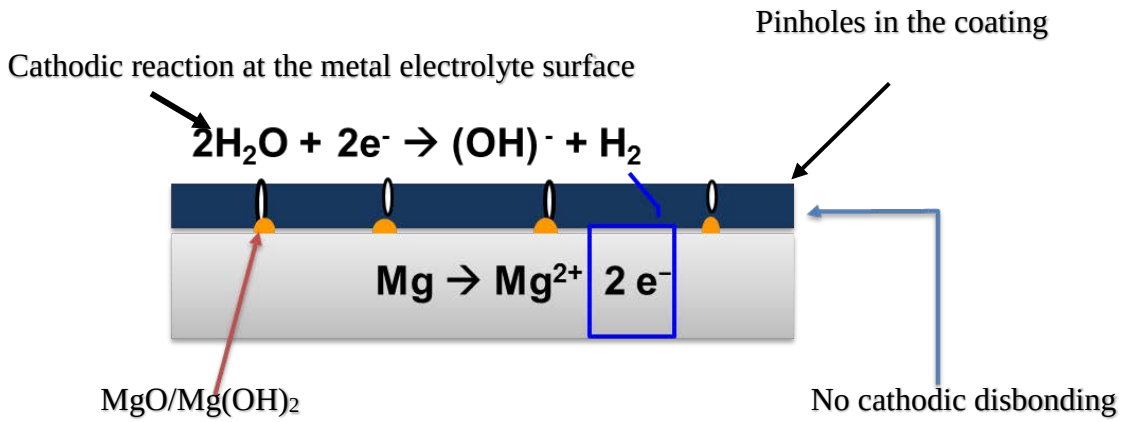

Figure 6.7 Schematic diagram of corrosion attack mechanism on AZ91 magnesium alloy sample coated with 0.1 aniline and 0.3 M sodium salicylate electrolyte.

The schematic diagram in Fig 6.7 explains the mechanism of corrosion attack on AZ91 magnesium alloy coated with polyaniline. These samples were not pre-treated with 3 M NaOH solution. During the potentiodynamic polarisation test, pinholes in the surface of the polyaniline coating allowed corrosive electrolyte to penetrate the surface of the coating. The chloride-containing corrosive electrolyte reacted with the AZ91 magnesium alloy, resulting in a cathodic reaction that produced hydrogen gas and OH ions, as shown in Figure 6.7. However, it was evident that the polyaniline coating was still attached to the surface of the metal substrate.

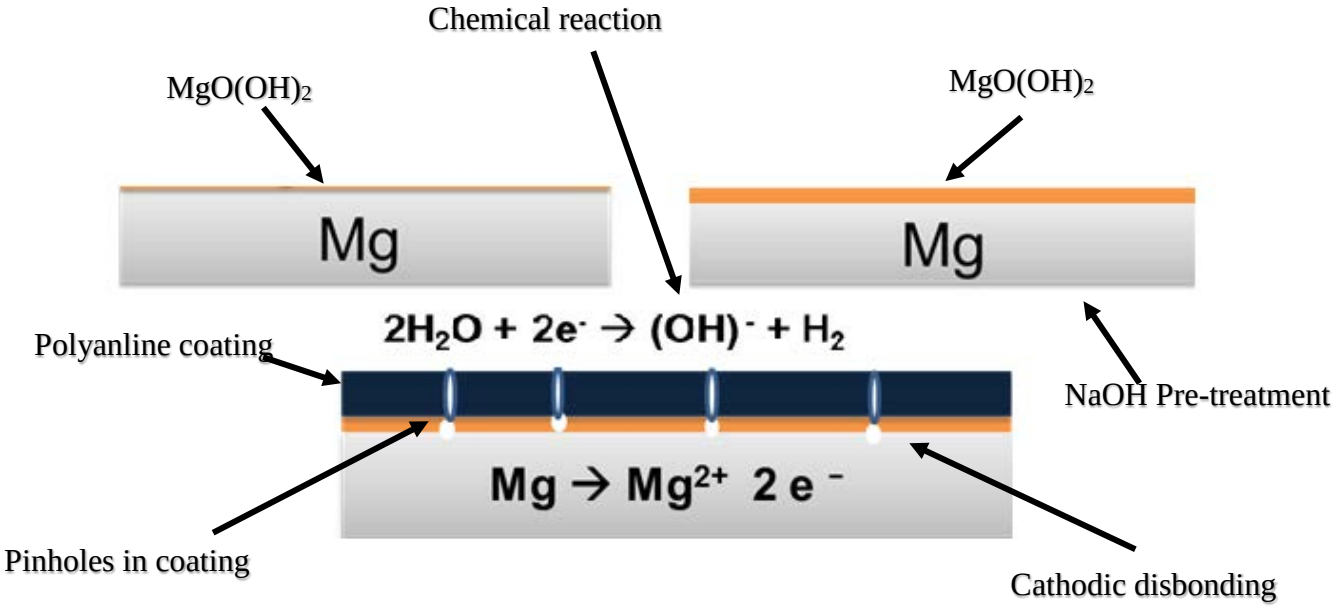

Figure 6.8 Schematic diagram of mechanism of corrosion attack on AZ91 magnesium alloy pre-treated with 3 M NaOH and coated with 0.1 aniline and 0.3 M sodium salicylate electrolyte

The mechanism in Figure 6.8 explains the systemic failure/delamination of the polyaniline coating on the AZ91 magnesium alloy. These samples were pre-treated with 3 M NaOH solution. The pinholes in the polyaniline coating allowed chloride-containing electrolyte to spread through under the polyaniline coating and react with $MgO/Mg(OH)_2$. The $MgO/Mg(OH)_2$ is an alkaline layer and can be easily dissolved in

the chloride-containing solution. Hence, on the basis of the dissolution of MgO /$Mg(OH)_2$, it can be suggested that delamination of the polyaniline coating occurs due to disbondment of the polymer coating and metal substrate.

6.4 Summary

- 3 M NaOH pre-treatment enhances polymer coating formation and passivation
- Pre-treatment was conducted at −750 mV and −185 mV constant potentials
- During the cyclic voltammetry polymerisation of polyaniline coating, the current density increased with increasing numbers of cycles
- Coating performance was investigated using potentiodynamic polarisation in a chloride-containing environment
- The polyaniline coating protected the alloy from corrosion; however, the coating obtained at five cycles without pre-treatment provided almost the same degree of protection as that obtained at 15 cycles with pre-treatment
- The results suggest that alkaline pre-treatment is not a good option for enhancing coating formation and passivation

CHAPTER 7 Conclusion

The corrosion performance of AZ91 magnesium alloy was enhanced by coating it with polyaniline. Two oxidizing agents of different pH, sodium salicylate and potassium hydroxide, were used with aniline to coat polyaniline on AZ91 magnesium alloy. The electrolyte containing potassium hydroxide (KOH; alkaline) and sodium salicylate ($C_7H_5NaO_3$; acidic) showed a different anodic current peak during cyclic voltammetry coating. Based on the anodic peak current density, it can be said that the oxidation of aniline in the alkaline electrolyte was significantly lower compared to that in the acidic electrolyte. Hence, it can be said that sodium salicylate is a better polymerisation agent than potassium hydroxide for aniline polymerisation on AZ91 magnesium alloy.

Pre-treatment in 3 M NaOH solution using a potentiostatic method was conducted to enhance the passivation and coating formation of the AZ91 magnesium alloy. Pre-treatment was done at −195 mV. The coatings formed on the surfaces of the alkaline pre-treated samples showed no visible pores. However, after potentiodynamic polarisation, the polyaniline coating exhibited delamination. The samples also showed white corrosion products, which suggests that alkaline pre-treatment is not suitable in the electropolymerisation of aniline on AZ91 magnesium alloy. The study also suggests that the polymer coating and oxide/hydroxide layer had very poor bonding and, hence, did not perform well during polarisation tests.

The performance of the electrodeposition of polyaniline (acidic electrolyte) was done by two electrochemical methods: cyclic voltammetric and galvanostatic. The coating obtained by the cyclic voltammetry technique showed a corrosion current (i_{corr}) of ~0.19 $\mu A/cm^2$ in 0.5 g/l NaCl solution. However, the coating done by the galvanostatic

technique showed better performance, with a corrosion current (i_{corr}) of ~0.081 µA/cm^2. The corrosion rates of the AZ91 magnesium alloy were 0.34 and 0.113 mpy for the cyclic voltammetry and galvanostatic techniques, respectively. The galvanostatic coatings were made at current densities of 14, 18 and 20 mA/cm^2, with the best corrosion protection performance obtained at 20 mA/cm^2.

Further work may include:

- Double layer PANI coating to reduce the chances of pinholes in the polymer layer.
- Long term (Multiple cycles i.e. 25, 50, 75 and 100) cyclic voltammetry coating to enhance the performance of the coating layer.
- Low current density galvanostatic coating for extended elapsed time to improve the corrosion resistance of the polyaniline coating.

References

Luo, A. (2013). “Magnesium casting technology for structural applications.” *Journal of magnesium and alloys*, 1, 2-22.

Hirsch, J. and Al-Samman, T. (2013). “Superior light metals by texture engineering: Optimized aluminium and magnesium alloys for automotive applications.” *Acta materials,* 61, 818-843.

Dobrzanski, L.A., Tanski, T., Cizek, L. and Brytan, Z. (2007) “Structure and properties of magnesium cast alloys.” *Journal of materials processing technology*, 192-193, 567-574.

Mordike, B.L. and Ebert, T. (2001) “Magnesium, Properties — applications — potential.” *Materials Science and Engineering.* A302, 37–45.

Easton, M., Beer, A., Barnett, M., Davies, C., Dunlop, G., Durandet, Y., Blacket, S., Hilditch, T., and Beggs, P. (2008) “Magnesium alloy applications in automotive Structures.” Vol. 60 No. 11, JOM, 57-60.

Kulekei, M. K., (2008) “Magnesium and its alloys applications in automotive industry.” *International Journal Advance Manufacturing Technology*, 39, 851-865.

Feng, J., Chen, Y., Liu, X., Liu. T., Zou, L., Yuting, W., Ren, Y., Fan, Z., Lv, Y., and Zhang, M., (2013) “In-situ hydrothermal crystallization $Mg(OH)_2$ films on magnesium alloy AZ91 and their corrosion resistance properties.” *Materials Chemistry and Physics*, 143, 322-329.

Craig, G. (1998) “Use of WE-43A-T6 Magnesium in the MD600 Helicopter Drive System.” IMA proceedings; International magnesium association, Vol 19-23.

Ghali, E. (2010) “Corrosion Resistance of Aluminum and Magnesium Alloys Understanding, Performance, and Testing.” John Wiley & Sons, Inc., Hoboken, New Jersey.

Ghali, E., Dietzel, W., and Kainer, K. (2004) “General and Localized Corrosion of Magnesium Alloys: A Critical Review.” *Journal of Material Engineering and Performance.* 13, 7-23.

Ambat R, Aung, N.N. and Zhou, W. (2000) “Studies on the influence of chloride ion and pH on the corrosion and electrochemical behaviour of AZ91D magnesium alloy.” *Journal of Applied Electrochemistry,* 30, 865-874.

Fontana, M. G. (1987). “Corrosion engineering” 20th reprint 2016, India; McGraw-Hill Book Company.

Gospodinova, N and Terlemezyan, L. (1998) Conducting polymers prepared by oxidative polymerisation: Polyaniline.” *Prog. Polym. Sci*., 23, 1443–1484.

Schab-Balcerzak, Ewa. (2011), “Electropolymerization” Rijeka, Croatia InTech, 77-96.

Camalet, J.-L., Lacroix, J.-C., Dung N.T, Aeiyach, S., Pham, M.C., Petitjean, J., and Lacaze, P.-C., (2000) “Aniline electropolymerization on platinum and mild steel from neutral aqueous media.” *Journal of Electroanalytical Chemistry*, 485, 13-20.

Hongbin, Lu., Zhou, Y., Vongehr S., Hu, K., and Xiangkan, M. (2011) “Electropolymerization of PANI coating in nitric acid for corrosion protection of 430 SS.” *Synthetic Metals,* 161, 1368-1376.

Masdarolomoor, F. (2006) “Noval nanostructured Conducting Polymer System Based on Sulfonnated Polyaniline.” PhD Thesis, University of Wollongong

Zhang, Y., Shao, Y., Zhang, T., Meng, G., and Wang, F (2013) “High corrosion protection of a polyaniline/organophilic montmorillonite coating for magnesium alloys” *Progress in Organic Coatings,* 76, 804-811.

Holness, R.J.; Williams, G.; Worsley, D.A.; and McMurray, H.N. (2005) “Polyaniline inhibition of corrosion-driven organic coating cathodic delamination of iron” *J. Elecrochem. Soc*. 152, 73–81

Guo X.W., Jiang, Y.F., Zhai C.Q., Lu. C., and Ding W.J. (2003) “Preparation of even polyaniline film on magnesium alloy by pulse potentiostatic method” *Synthetic Metals* 136-136, 169-170

Jude O. Iroh, and Wencheng Su. (2000) “Corrosion performance of polypyrrole coating applied to low carbon steel by an electrochemical process.” *Electrochimica Acta,* 46, 15–24

Kazum, O., and Kannan, M. B. (2013). “Galvanostatic polymerisation of aniline on steel: Improving the coating performance in chloride-containing environment.” *Synthetic Metals,* 180, 54-58.

Pawar, P., Gaikawad, A.B., and Patil, P.P. (2006). “Electrochemical synthesis of corrosion protective polyaniline coatings on mild steel from aqueous salicylate medium”. *Science and Technology of Advanced Materials*, 7, 732-744.

Cao, F., Song G-Ling., and Atrens, A. (2016) “Corrosion and passivation of magnesium alloys: A review” *Corrosion Science,* 111, 835-845

Williams, G., Dafydd, H. L., and Grace, R. (2013). “The localised corrosion of Mg alloy AZ31 in chloride containing electrolyte studied by a scanning vibrating electrode technique.” *Electrochimica Acta,* 109, 489-501.

Kannan, M. B., and Dietzel, W. (2012). “Pitting-induced hydrogen embrittlement of magnesium–aluminum alloy.” *Materials & Design*, 42, 321-326.

Shi, Z., Xueshan Jia, J., Atrens, A. (2012) “Galvanostatic anodic polarisation curves and galvanic corrosion of high purity Mg in 3.5% NaCl saturated with $Mg(OH)_2$” *Corrosion Science,* 60, 296-308

Atrens, A., Liu, M., and Zainal Abidin, N. (2011) “Review: Corrosion mechanism applicable to biodegradable magnesium implants” *Materials Science and Engineering,* 17, 1609-1636.

Kannan, M. B., Dietzel, W. Blawert, C., Atrens, A. and Lyon, P. (2008). “Stress corrosion cracking of rare-earth containing magnesium alloys ZE41.” *Material Science and Engineering,* 480, 529-539.

Kannan, M. B., Dietzel, W., Zeng, R., Zettler, R., and Dos Santos, J.F. (2007). “A study on the SCC susceptibility of friction stir welded AZ31 Mg sheet.” *Materials Science and Engineering:* A, 460-461, 243-250.

Williams, G., and Grace, R. (2011). “Chloride-induced filiform corrosion of organic-coated magnesium.” *Electrochimica Acta*, 56, 1894-1903.

Sayyah, S.M. and Azooz, R.E. (2016). “Electrosynthesis and characterization of adherent poly(2-aminobenzothiazole) on Pt-electrode from acidic solution.” *Arabian Journal of Chemistry,* 9, 675-586.

Sapurina, I. Yu. and Shishov, M.A. (2012) “Oxidative Polymerization of Aniline:Molecular Synthesis of Polyaniline and the Formation of Supramolecular Structures, In: New polymers for special applications” InTech, Croatia, 251-312

Otsuka, T. (2012). “Corrosion Protection of Steel by Conductive Polymer.” *International Journal of Corrosion,* 1-8

Stejskal, J., Sapurinab, I., and Trchova, M. (2010). “Polyaniline nanostructures and the role of aniline oligomers in their formation.” *Progress in Polymer Science,* 35, 1420-1481.

Gvozdenovi, M. M., and Grgur. B. N. (2009). “Electrochemical polymerization and initial corrosion properties of polyaniline-benzoate film on aluminum.” *Progress in Organic Coatings,* 65, 401–404.

Sorkhabi H. A., and Rafizadeh S.H. (2004) “Effect of coating time and heat treatment on structures and corrosion characteristics of electroless Ni–P alloy deposits” *Surface and Coatings Technology* 176, 318-326

Yantapure M., Deshpande, P., and Vagge S. (2015) “Effect of current density and deposition time on galvanostatic phosphating of low carbon steel” *U.P.B. Sci. Bull., Series B, Vol. 77*, 174-184

Kaplin, D.A., and Qutubuddin, S. (1995). “Electrochemically synthesized polypyrrole films: effects of polymerization potential and electrolyte type.” *Polymer*. 36, 1275-1285.

Singh, R.N., Lal, B., and Malviya, M. (2004). “Electrocatalytic activity of electrodeposited composite films of polypyrrole and $CoFe_2O_4$ nanoparticles towards oxygen reduction reaction.” *Elctrochimica Acta*, 49, 4605-4612.

Wang, L., Li, X., and Yang, Yu. (2001). “Preparation, properties and application of polypyrrole.” *Reactive & Functional Polymers*, 47, 125-139.

Abou-Elenien, G.M., El-Maghraby, A.A., and El-Abdullah, G.M. (2004). “Electrochemical relaxation study of polythiophene as conducting polymer (I).” *Synthetic Metals*, 146, 109–119.

Vered, P., Katz, E., Lioubashevski, O., and Itamar, W. (2001) “Layered Polyelectrolyte Films on Au Electrodes: Characterization of Electron-Transfer Features at the Charged Polymer Interface and Application for Selective Redox Reactions.” *Langmuir,* 17, 1110-1118

Breslin, C.B., Fenelon, A.M., and Conroy. K.G. (2005) “Surface engineering: corrosion protection using conducting polymers.” *Materials and Design,* 26, 233–237

Kang, Z., Sang, J., Shao, M., and Li, Y. (2009) “Polymer plating on AZ31 magnesium alloy surface and film evaluation of corrosion property.” *Journal of Materials Processing Technology,* 209, 4590-4594.

Ocon, P., Cristobal, A.B., Herrasti, P., and Fatas, E. (2005) “Corrosion performance of conducting polymer coating applied on a mild steel.” *Corrosion science,* 47, 649-662.

Sazou, D., Kourouzidou, M., and Pavlidou, E. (2007). "Potentiodynamic and potentiostatic deposition of polyaniline on stainless steel: Electrochemical and structural studies for a potential application to corrosion control." *Electrochimica Acta,* 52, 4385-4397.

Borole, D.D., Kapadi, U.R., Mahulikar, P.P., and Hundiwali. D.G. (2006). "Synthesis and characterization of poly (aniline-co-o-anisidine-co-o-toluidine) thin films in inorganic and organic supporting electrolytes." *Journal of Material Science,* 41, 1983-1990.

Martyak, N. M., McAndrew, P., McCaskie, J. E., and Julien. D. (2002). "Electrochemical polymerization of aniline from an oxalic acid medium." *Progress in Organic Coating,* 45, 23-32.

Benyaich, A., Deslouis, C., El Moustafied, T., Musiani, M. M. and Tribollet, B. (1996). "Electrochemical properties of PANI films for different counter-ions in acidic pH analysed by impedance techniques." *Electrochimica Acta,* 41, 1781-1785.

Biallozor, S., and Kupniewska, A. (2005). "Conducting polymers electrodeposition on active metals." *Synthetic Metals,* 23, 443-449.

Raotole, P., Patil, PP., and Gaikwad, Ab. (2013). "Polypyrrole coatings on low carbon steel from aqueous oxalate solution." *Int. Journal of Emg. Tech and Adv.* 11, 68-73.

Heydari, M. H., Zebhi, H., Farhadi, K., Moghadam, P. N. (2016). "Electrochemical synthesis of nanostructure poly(3-aminobenzoic acid), polyaniline and their bilayers on 430SS and their corrosion protection performances." *Synthetic metals,* 220, 78-85.

Dalmolin, C., Canobre, SC., Biaggio, SR., Rocha-Filho, RC., and Bocchi. N. (2005) "Electropolymerization of polyaniline on high surface area carbon substrates." *Journal of Electroanalytical Chemistry,* 578, 9-15.

Cascalheira, A.C., Aeiyach, S., Lacaze, P.C., Abrantes, L.M. (2003). "Electrochemical synthesis and redox behaviour of polypyrrole coatings on copper in salicylate aqueous solution." *Electrochimica Acta*, 48, 2523-2529

Martins, N.C.T., Moura e Silva, T., Montemor, M.F., Fernandes, J.C.S., Ferreira, M.G.S. (2008). "Electrodeposition and characterization of polypyrrole films on aluminium alloy 6061-T6." *Electrochimica Acta,* 52, 4754-4663.

Hu, RG., Zhang, S., Bu, JF., Lin, CJ., and Song, GL. (2012). “Recent progress in corrosion protection of magnesium alloys by organic coatings.” *Progress in Organic Coatings,* 73, 129–141.

Sathiyanarayanan, S., Syed SA., and Venkatachari, G. (2006). “Corrosion resistant properties of polyaniline–acrylic coating on magnesium alloy.” *Applied Surface Science,* 253, 2113–2117.

Rout, TK., Jha, G., Singh, AK., Bandyopadhyay, N., and Mohanty. O.N. (2003). “Development of conducting polyaniline coating: a novel approach to superior corrosion resistance.” *Surface and Coatings Technology,* 167, 16-24.

Radhakrishnan, S., Siju, CR., Mahanta, D., Patil, S., and Madras, G. (2009). “Conducting polyaniline–nano-TiO_2 composites for smart corrosion resistant coatings”. *Electrochimica Acta,* 54, 1249-1254.

Sambyal, P., Ruhi, G., Dhawan, R., and Dhawan. SK. (2016). “Designing of smart coatings of conducting polymer poly(aniline-co-phenetidine)/SiO2 composites for corrosion protection in marine environment.” *Surface and Coating Technology,* 303, 362-371.

Luo, Y., Sun, Y., Lv, J., Wang, X., Li, J., Wang, F., (2015) “Transition of interface oxide layer from porous $Mg(OH)_2$ to dense MgO induced by polyaniline and corrosion resistance of Mg alloy therefrom” *Applied Surface Science*, 328, 247-254.

Hara, N., Kobayashi, Y., Kagaya, D., and Akao, N. (2007). “Formation and breakdown of surface films on magnesium and its alloys in aqueous solutions.” *Corrosion Science,* 49, 166-175.

LI, LL., Cheng, YL., Wang, HM., and Zhang, Z. (2008). “Anodization of AZ91 magnesium alloy in alkaline solution containing silicate and corrosion properties of anodized films.” *Trans. Nonferrous Met. Soc. China.* 18, 722-727.

Arenas, MA., Bajos, LG., De Damborenea, JJ., and Ocon, P. (2008). “Synthesis and electrochemical evaluation of polypyrrole coatings electrodeposited onto AA-2024 alloy.” *Progress in Organic Coating,* 62, 79-86.

Liu, XX., Zhang, L., Li, YB., Bian, LJ., Su, Z., and Zhang, LJ. (2005) .“Electropolymerization of aniline in aqueous solutions at pH 2 to 12.” *Journal of Materials Science*, 40. 4511-4515

Kirkland, NT., Williams, G., Birbilis, N. (2012). “Observations of the galvanostatic dissolution of pure magnesium.” *Corrosion Science.* 65, 5-9.

Prejza, J., Lundstrom, I., and Skotheim. T. (1982). “Electropolymerization of Pyrrole in the Presence of Fluoborate.” *Journal of Electrochemical Society*, 1685-1688.

Fang, J., Xu, K., Zhu, L., Zhou, Z., and Tang, H. (2007). “A study on mechanism of corrosion protection of polyaniline coating and its failure.” *Corrosion Science*, 49, 4232-4242.

Bakkar, A., and Neubert, V. (2007). “Electrodeposition onto magnesium in air and water stable ionic liquids: From corrosion to successful plating.” *Electrochemistry Communications*. 9, 2428–2435.

Ezhilselvi, V., Nithin, J., Balaraju, JN., and Subramanian. S. (2016). “The influence of current density on the morphology and corrosion properties of MAO coatings on AZ31B magnesium alloy.” *Surface & Coatings Technology,* 288, 221–229.

Wang, T., and Tan, YJ. (2006). “Understanding electrodeposition of polyaniline coatings for corrosion prevention applications using the wire beam electrode method.” *Corrosion Science*, 48, 2274–2290.

Babaiee, M., Pakshir, M., and Hashemi, B. (2015). “Effects of potentiodynamic electropolymerization parameters on electrochemical properties and morphology of fabricated PANI nanofiber/graphite electrode.” *Synthetic Metals,* 199, 110-120.

Hasanov, R., and Bilgic, S. (2009). “Monolayer and bilayer conducting polymer coatings for corrosion protection of steel in 1 M H_2SO_4 solution.” *Progress in Organic Coatings*, 64, 435–445.

Samaniego, A., Gusieva, K., Llorente, I., Feliu. S., and Birbilis, N. (2014). “Exploring the possibility of protective surface oxides upon Mg alloy AZ31 via lutetium additions.” *Corrosion Science,* 89, 101-110.

Feliu, S., Maffiotte, C., Samaniego, A., Galván, JC., and Barranco, V. (2011). “Effect of the chemistry and structure of the native oxide surface film on the corrosion properties of commercial AZ31 and AZ61 alloys.” *Applied Surface Science*, 257, 8558-5868.

Taheri, M., Phillips, RC., Kish JR., and Botton. GA. (2012). “Analysis of the surface film formed on Mg by exposure to water using a FIB cross-section and STEM–EDS.” *Corrosion Science,* 59, 222-228.

Czerwinski. F., (2011). “Magnesium alloys- Corrosion and surface treatment” Rijeka, Croatia InTech, 27-40.

Costa. M., (1997) “Toxicity and Carcinogenicity of Cr (VI) in Animal Models and Humans”, *Critical Reviews in Toxicology*, 27:5, 431-442

Rohwerder, M., and Michalik, A., (2007), “Conducting polymers for corrosion protection: What makes the difference between failure and success?” *Electrochimica Acta* 53:3, 1300-1313.

Searle. J. R., Wilson B. P., Yliniemi K., Worsley D. A., and McMurray, H. N (2015) “The Use of 3D-SVET for the Examination of Plasticized PVC Coatings: Effect of Deformation and UV Irradiation on Barrier Properties”. *The Electrochemical Society* 64:26, 69-80.

Shaw B. A. (2003) Corrosion resistance of magnesium alloys, *ASM Handbook, Volume 13A,* 692-696